THE METHOD OF DISTRIBUTED VOLUMETRIC SOURCES FOR FORECASTING THE TRANSIENT AND PSEUDO-STEADY STATE PRODUCTIVITY OF MULTIPLE TRANSVERSE FRACTURES INTERSECTED BY A HORIZONTAL WELL

A Thesis

by

DIANGENG FAN

Submitted to the Office of Graduate Studies of
Texas A&M University
in partial fulfillment of the requirements for the degree of

MASTER OF SCIENCE

December 2010

Major Subject: Petroleum Engineering

THE METHOD OF DISTRIBUTED VOLUMETRIC SOURCES FOR FORECASTING THE TRANSIENT AND PSEUDO-STEADY STATE PRODUCTIVITY OF MULTIPLE TRANSVERSE FRACTURES INTERSECTED BY A HORIZONTAL WELL

A Thesis

by

DIANGENG FAN

Submitted to the Office of Graduate Studies of
Texas A&M University
in partial fulfillment of the requirements for the degree of

MASTER OF SCIENCE

Approved by:

Chair of Committee,	Peter P. Valkó
Committee Members,	Christine Ehlig-Economides
	Christopher Pope
Head of Department,	Stephen A. Holditch

December 2010

Major Subject: Petroleum Engineering

ABSTRACT

The Method of Distributed Volumetric Sources for Forecasting the Transient and Pseudo-steady State Productivity of Multiple Transverse Fractures Intersected by a Horizontal Well. (December 2010)

Diangeng Fan, B.S., University of Science and Technology of China

Chair of Advisory Committee: Dr. Peter P. Valkó

This work of well performance modeling is focused on solving problems of transient and pseudo-steady state fluid flow in a rectilinear closed boundaries reservoir. This model has been applied to predict and to optimize gas production from a horizontal well intercepted by multiple transverse fractures in a bounded reservoir, and it also provides well-testing solutions.

The well performance model is designed to provide enhanced efficiency with the same reliability for pressure transient analysis, and well performance prediction, especially in complex well fracture configuration. The principle is to simplify the calculation of the pressure response to an instantaneous withdraw, which happens in other fractures, within a shorter computational time. This pressure response is substituted with the interaction between the two whole fractures. This method is validated through comparison to results of rigorous Distributed Volumetric Sources (DVS) method in simple symmetric fracture configuration, and to results of field production data for complex well/fracture configuration of a tight gas reservoir. The results show a good agreement in both ways.

This model indicates the capability to handle the situations, such as: various well drainages, asymmetry of the fracture wings, and curved horizontal well. The advantage of this well performance model is to provide faster processing - reducing the computational time as the number of fractures increase. Also, this approach is able to be applied as an optimization and screening tool to obtain the best fracture configurations for reservoir development of economically marginal fields, in terms of the number and dimensions of fractures per well, also with external economic and operational constraints.

DEDICATION

To my family and all my friends who have always stood by me

ACKNOWLEDGMENTS

I would like to express my deepest gratitude and appreciation to my advisor and committee chair, Dr. Peter P. Valkó, for believing in me and helping me out when everything looked bleak. His constant encouragement and creative ideas have always motivated me to work beyond my ability.

I would also like to thank Dr. Christine Ehlig-Economides and Dr. Christopher Pope for serving as my committee member. Thank you for your effort.

I would like to thank the Department of Petroleum Engineering at Texas A&M University for sponsoring me during my endeavor for a master's degree in petroleum engineering.

Finally, thanks to my mother and father for their encouragement and love.

TABLE OF CONTENTS

Page

NOMENCLATURE

Variables

A	=	reservoir drainage area, ft^2
c_t	=	total compressibility, psi^{-1}
c_{trad}	=	conversion factor
c_x	=	position of the center of the source in x direction, ft
c_y	=	position of the center of the source in y direction, ft
c_z	=	position of the center of the source in z direction, ft
f	=	1D solution to the flow equation
J_D	=	dimensionless productivity index
$J_{D,\ trand}$	=	traditional definition of dimensionless productivity index
k	=	permeability, reference permeability, md
k_x	=	directional permeability in x direction, md
k_y	=	directional permeability in y direction, md
k_z	=	directional permeability in z direction, md
p	=	pressure, psi
p_i	=	initial pressure, psi
p_{wf}	=	well flowing pressure, psi
$p_{\delta D}$	=	dimensionless pressure due to instantaneous source
PI	=	productivity index, STB/d/psi
p_{uD}	=	dimensionless pressure due to continuous source
t	=	time
t_D	=	dimensionless time

t_{DA}	=	dimensionless time with regard to reference drainage volume
$t_{DA,\ trad}$	=	dimensionless time with regard to fracture half-length
w_x	=	source width in x direction, ft
w_y	=	source width in y direction, ft
w_z	=	source width in z direction, ft
x_D	=	dimensionless length in x direction, x/xe
x_e	=	length of outer box, ft
y_D	=	dimensionless width in y direction, y/ye
y_e	=	width of the outer box, ft
z_D	=	dimensionless height in z direction, z/ze
z_e	=	height of the outer box, ft

Greek Symbols

ϕ	=	porosity, fraction
μ	=	viscosity, cp

LIST OF FIGURES

Page

Page

Page

Page

LIST OF TABLES

Page

CHAPTER I

INTRODUCTION

1.1 General Background

In an era of declining production and increasing demand, economically producing gas from unconventional sources is the next level of the fossil-fuel recovery challenge. The mammoth volume and long-term potential of coalbed methane (CBM), tight gas, and hydrate resources are driving technical progress. Attractive gas prices in North America and unprecedented interest in world markets promise to bring unconventional gas into the forefront of our energy future (Garbut, 2004).

A considerable amount of gas is currently produced from unconventional Mississippian organic-rich shale gas fields such as the Barnett, the Fayetteville or the Bakken formations. Several tight-gas sand formations (e.g., Bossier, Cotton Valley, Lobo, Vicksburg, etc.) also provide valuable resources to be exploited.

These formations are extremely low porosity and permeability reservoirs. They must be effectively and efficiently hydraulically fracture stimulated to produce at commercially economic production rates. Hydraulic fracture and horizontal well completions are intended to provide a larger surface area for fluid withdrawal, and thus improve the production.

This thesis follows the style of *SPE Journal.*

For the unconventional resource formations, it is difficult to design an optimum fracture treatment and describe production behavior by a regular reservoir simulator. Over the past decades, different techniques were developed to solve single phase, slight compressible flow problems for a complex well fracture system. Beginning with Gringarten and Ramey (1973), they applied appropriate instantaneous Green's and source functions, with the Newman's product method to solve unsteady reservoir flow problems for a slightly compressible fluid. Then Cinco-Ley et al. (1978) divided the fracture flux a stepwise distribution in time and space to analyze the transient behavior. These methods use the point source integrated over a line or a surface, so the solution is based on these required reference points to perform calculations. Thus, they meet with a major disadvantage, which is the inherent singularity of the solution where the source is placed. The method of Distributed Volumetric Sources (DVS) was developed to remove this limitation by assuming every source, regardless of its size and dimensions, to contain a rectilinear volume inside the surrounding rectilinear porous media, instead of a source point. The DVS method also provides a faster and more reliable solution for the problems of transient and pseudosteady-state fluid flow in a reservoir with closed boundaries.

The solutions generated by DVS method, provides well testing pressure derivative, and the pressure derivative can be integrated over the time to provide the pressure response analytically to continuous volumetric source. The calculated pressure response will then be used to determine productivity index of a reservoir over a time period, which is an important indicator of well production capacity.

Furthermore, as the oil and gas industry is intended to explore lower quality reservoirs, which exhibit a low or even ultra low permeability, the transient flow

dominates and pseudosteady-state productivity calculations become more critical in prediction of the production behavior of the reservoir. The DVS method will fill this gap by providing the productivity index of a specific well completion scheme for both transient and pseudosteady-state flow.

1.2 Literature Review

In this chapter, an overview of previous work approaching the establishment of DVS method will be briefly summarized. The application of hydraulic fracture and microseismic hydraulic fracture monitoring will be presented.

1.2.1 Foundation Knowledge for DVS Method

In an early study by Gringarten and Ramey (1973), starting from the diffusivity equation, with some assumed boundary condition, the appropriate instantaneous Green's and source functions were first applied with the Newman's product method to solve unsteady reservoir flow problems for a slightly compressible fluid.

Then, Gringarten et al. (1975) combined older semilog analytical methods with the log-log type curve to analyze the transient pressure data of two cases: the infinite conductivity vertical fracture in a square drainage region; horizontally fractured well in an infinite medium.

Cinco-Ley et al. (1978) developed a mathematical model to analyze transient behavior for wells with a finite conductivity vertical fracture in a homogeneous reservoir. By assuming the fracture flux has a stepwise distribution in time and space, they used the method to divide the fracture into 2N equal segments, to divide the time into K different intervals. The solution is plotted as a curve pwf_D vs log t_D: for early time transient

pressure data, the type curve matching was procedure to analyze; for larger t_D, the semi-logarithmic pressure analysis was applied.

Cinco-Ley et al. (1975) also got an analytical solution derived for the unsteady flow of a slightly compressible fluid of a well with inclined fracture. Dimensionless pressure drop was evaluated from the solution. They also considered both the fully and partially penetrating situations.

The transient flow behavior of a vertical fractured well would exhibit four flow periods: Bilinear flow (Cinco-Ley et al., 1981), pseudo-linear flow and the pseudo-radial flow – which are separately under the influence of the different states of the fluid transfer between matrix and fractures: fracture dominated period, transition period and total system dominated period. For the flow periods: transient flow, bilinear flow, pseudo-linear flow and the pseudo-radial flow, the pressure data exhibit a straight line in a graph of pressure versus t1/8, t1/4, t1/2 and log t, respectively. The whole behavior could be correlated by the parameter dimensionless fracture conductivity (Cinco-Ley and Meng, 1988).

Pressure derivative technique was used simultaneously with the pressure to analyze wells with a finite conductivity fracture. Two cases were studied during the bilinear-flow period: the case without fracture skin or wellbore storage, and the case with fracture skin and wellbore storage. The uniqueness problem in type-curve matching could be reduced when use pressure derivative with pressure behavior type curves (Wong et al., 1986).

The mechanism of fluid flow in the reservoir can be determined through the knowledge of the potential distribution inside the reservoir. Azar-Nejad et al. presented a

new method “Discrete Flux Element”, which provided a general analytical solution to the diffusivity equation in two types of wellbore conditions: uniform potential and uniform flux inner boundary conditions (Azar-Nejad et al., 1996a) (Azar-Nejad et al., 1996b). Chen and Asaad (2005) analytically simplified productivity index equations to forecast the pseudosteady state horizontal well productivity within a consistent framework, also in the two types of wellbore conditions.

Valko and Economides (2002) introduced a novel variable called dimensionless Proppant Number. They pointed out the hydraulic fracture treatment sizes can be unified because they can be best characterized by the dimensionless Proppant Number, which determines the theoretically optimum fracture dimensions at which the maximum productivity or injectivity index can be obtained. With the dimensionless Proppant Number, technical constraints could be satisfied in such a way that the design departs from the theoretical optimum only to the necessary extent.

Meyer and Jacot (2005) used a reservoir fracture domain resistivity concept to present a new solution methodology for pseudosteady state behavior of a well with a finite conductivity vertical fracture. The solution is presented in the form of the dimensionless productivity index. They discussed the fundamental building blocks, effective wellbore radius, pseudo-skin functions and fracture skin. They improve the Gringarten’s dimensionless productivity solution for infinite conductivity vertical fractures in rectangular closed reservoirs.

1.2.2 Application of Hydraulic Fracture in Unconventional Gas Reservoir

In an era of declining production and increasing demand, economically producing gas from unconventional sources is the next level of the fossil-fuel recovery challenge.

The mammoth volume and long-term potential of coalbed methane (CBM), tight gas, and hydrate resources are driving technical progress. Attractive gas prices in North America and unprecedented interest in world markets promise to bring unconventional gas into the forefront of our energy future. (Garbut, 2004)

1.2.3 Microseismic Hydraulic Fracture Monitoring

A considerable amount of gas is currently produced from unconventional Mississippian organic-rich shale gas fields such as the Barnett, the Fayetteville or the Bakken formations. Several tight-gas sand formations (e.g., Bossier, Cotton Valley, Lobo, Vicksburg, etc.) also provide valuable resources to be exploited.

These formations are extremely low porosity and permeability reservoirs. They must be effectively and efficiently hydraulically fracture stimulated to produce at commercially economic production rates. Understanding the location and geometry of the created fractures and the area of pay affected by the fracture treatment is key to maximizing the value of the completion and reservoir management program.

Technology has progressed to the point that microseismic monitoring of hydraulic fracture stimulation can efficiently provide extensive diagnostic information on fracture development and geometry. Furthermore, an acquisition system coupled to a real-time processing software linked to a fit-for-purpose visualization package enables true real-time microseismic monitoring of hydraulic fracture treatments. (Le Calvez et al. 2007).

Using microseismic hydraulic fracture monitoring in real time can identify unwanted fracture-growth behavior, allowing the user to change the design on the fly. Real-time monitoring can then show how the alteration affected the overall treatment and ultimately if treatment was a success or not. If the treatment change was ineffective, then

another fracture-treatment alteration can be attempted and the results can be viewed real time to determine if it was successful (Baihly et al., 2009).

- Determine whether the fracture is getting out of zone or whether length extension is still occurring;
- Determine whether the isolation method has been used effectively;
- Determine whether fracture stages overlap, then either a stage is terminated early and then the subsequent fracture stage can begin, or a diversion technique can be applied to propagate the fracture in its designed fairway;
- Determine whether multiple fractures occur, then the stage can be pumped longer than designed
- If a fault exists, the stage can be terminated early
- Predict where microseisms should occur in relation to the fracture and make possible accurate interpretation of the significance of the microseismic events (Warpinski et al., 2001).

Figure 1 and **Figure 2** highlight the importance of real-time microseismic hydraulic fracture monitoring. These figures show 3D and map views, respectively, of a seven-fracture-stage horizontal well.

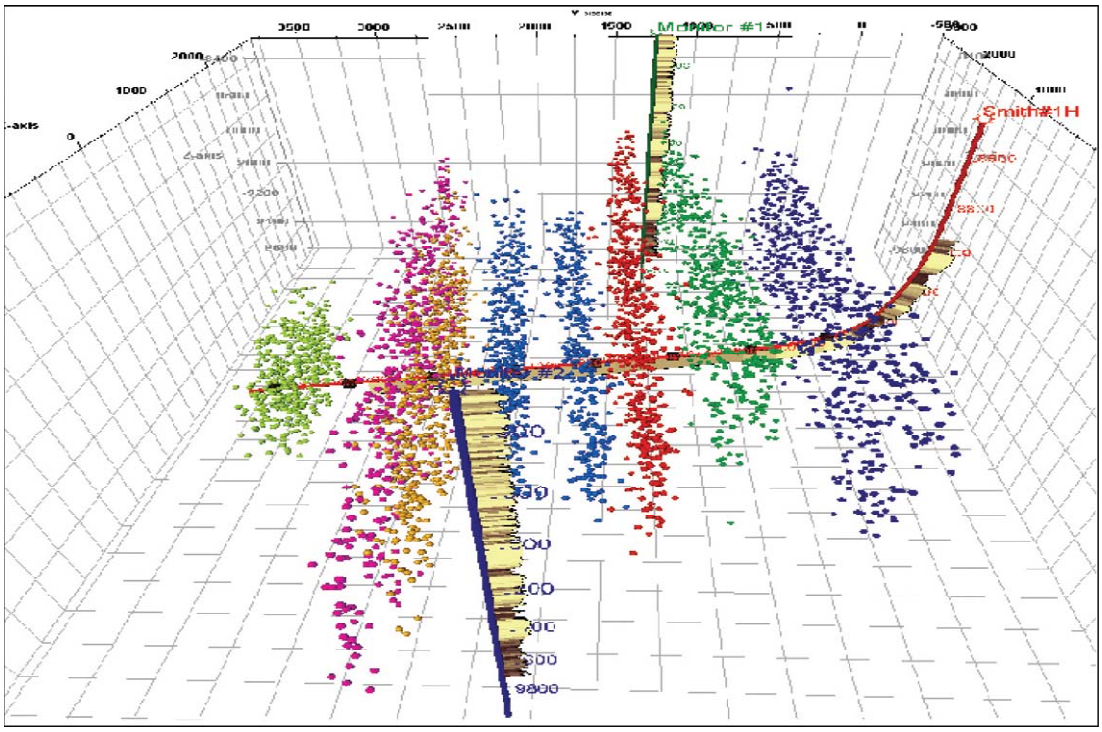

Figure 1 3D View of a Horizontal Well with Microseismic Results Colored by Stage

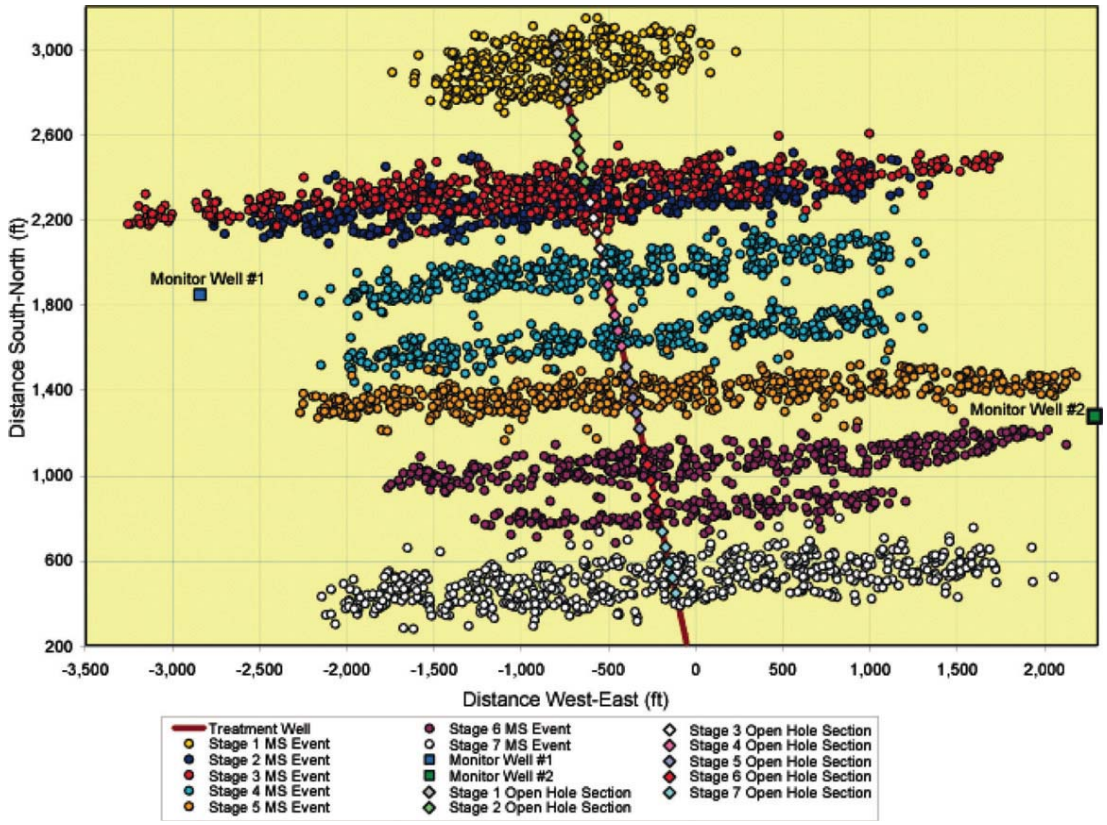

Figure 2 A Map View of a Horizontal Well with Microseismic Results Colored by Stage

Microseismic hydraulic fracture monitoring is having a major impact in how wells are being completed in tight sand reservoirs. This existing technology is being utilized in new and innovative ways to provide operators a clearer picture of the fracture development.

Wells in the Cotton Valley sand have to be hydraulically fractured to produce gas economically because of such low permeability. (Baihly et al., 2007)

Microseismic monitoring was used on both hydraulic fracture stages of the DCW I well. **Figure 3** and **Figure 4** show the length and height of the microseismic hydraulic fracture monitoring results of stages one and two, respectively. **Figure 5** shows the length

and height view of the combined microseismic results of both stages, whilst **Figure 6** shows the map view. This latter profile shows the length and width of the rock volume affected by the fracture. The microseismic dimension results for both stages can be found in **Table 1**. **Table 1** also lists the interpreted microseismic length and height. The interpreted microseismic dimensions differ from the total microseismic dimensions as outlying microseismic events have been removed.

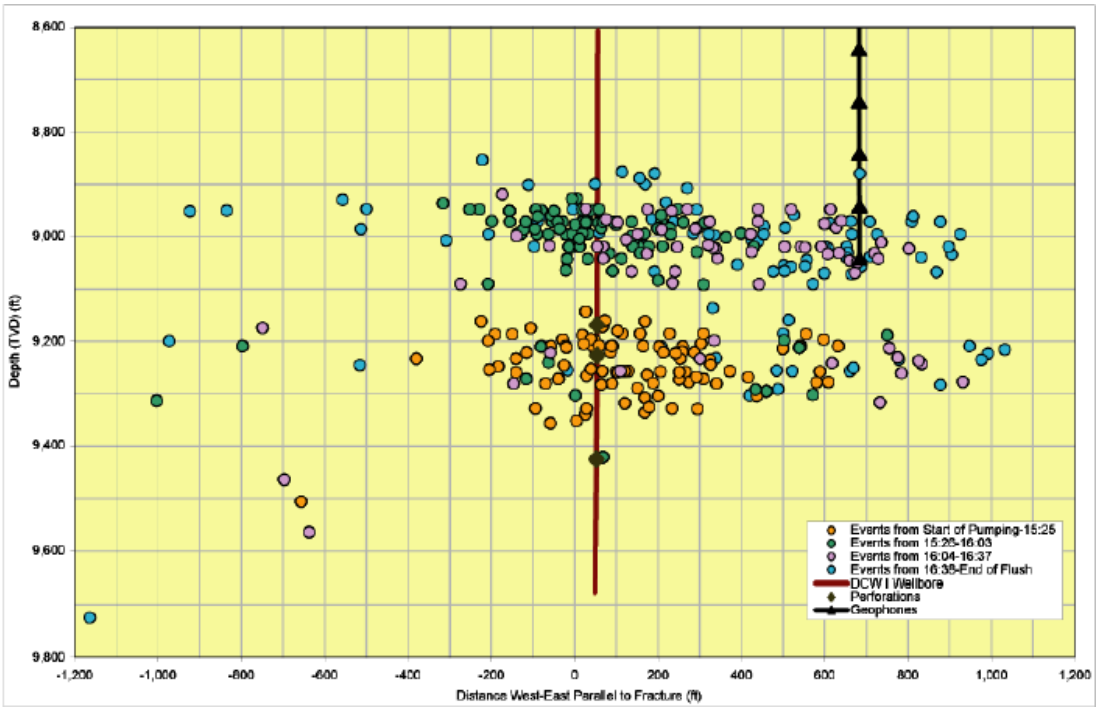

Figure 3 DCW I Stage One Microseismic Results (View Parallel to Fracture)

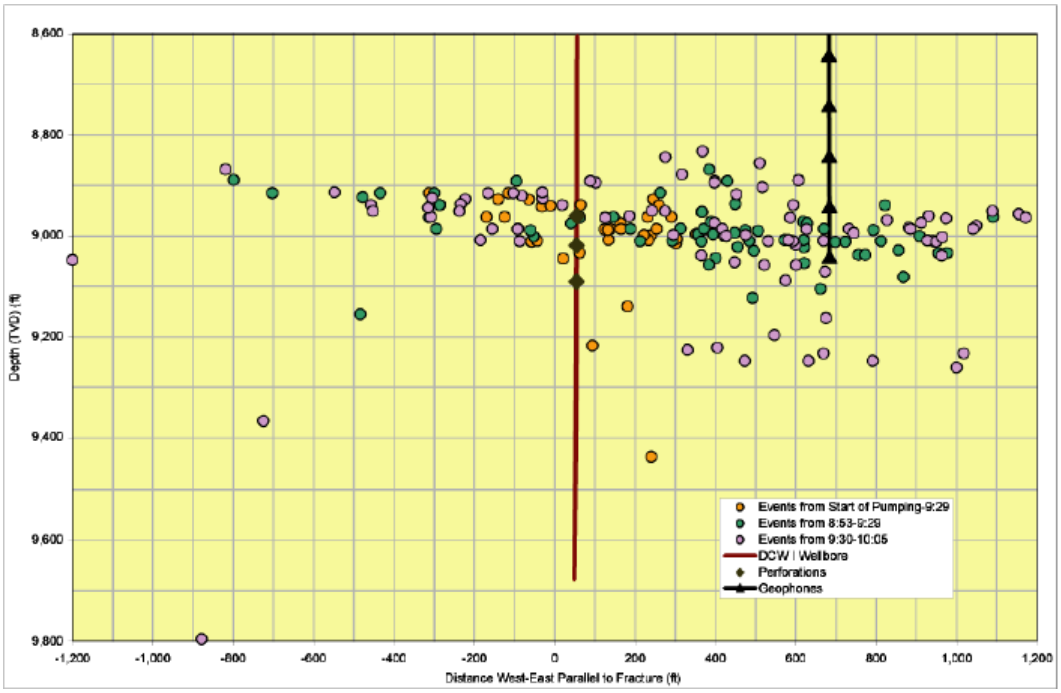

Figure 4 DCW I Stage Two Microseismic Results (View Parallel to Fracture)

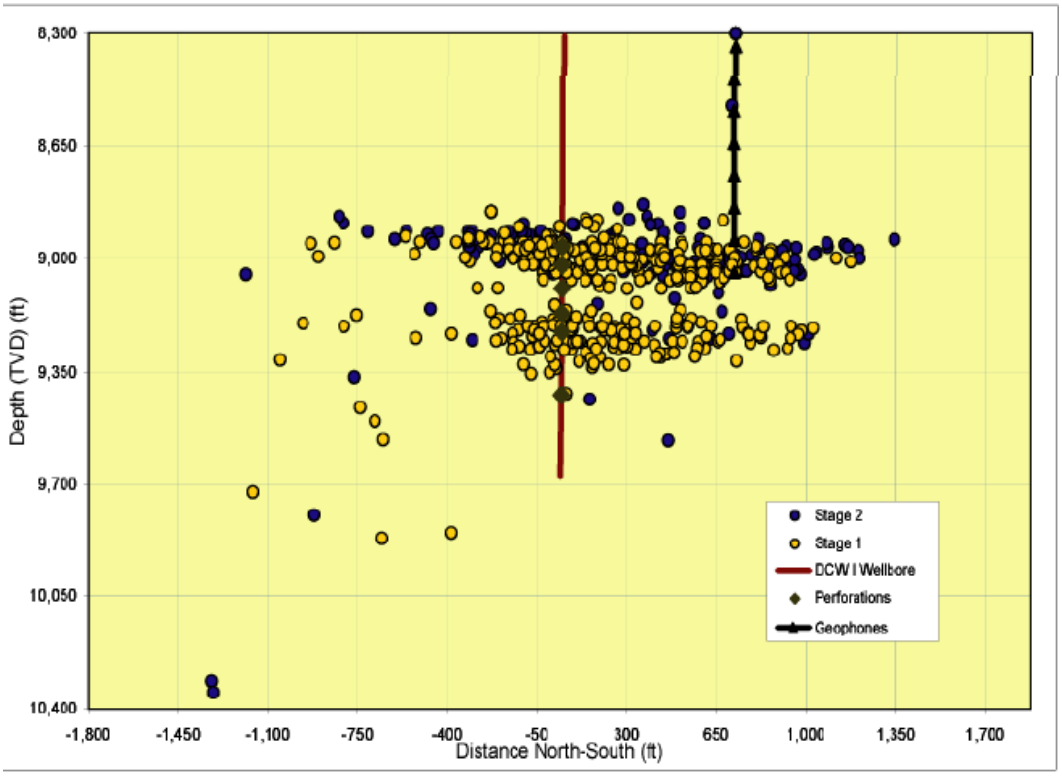

Figure 5 DCW I Both Stages Microseismic Results (View Parallel to Fracture)

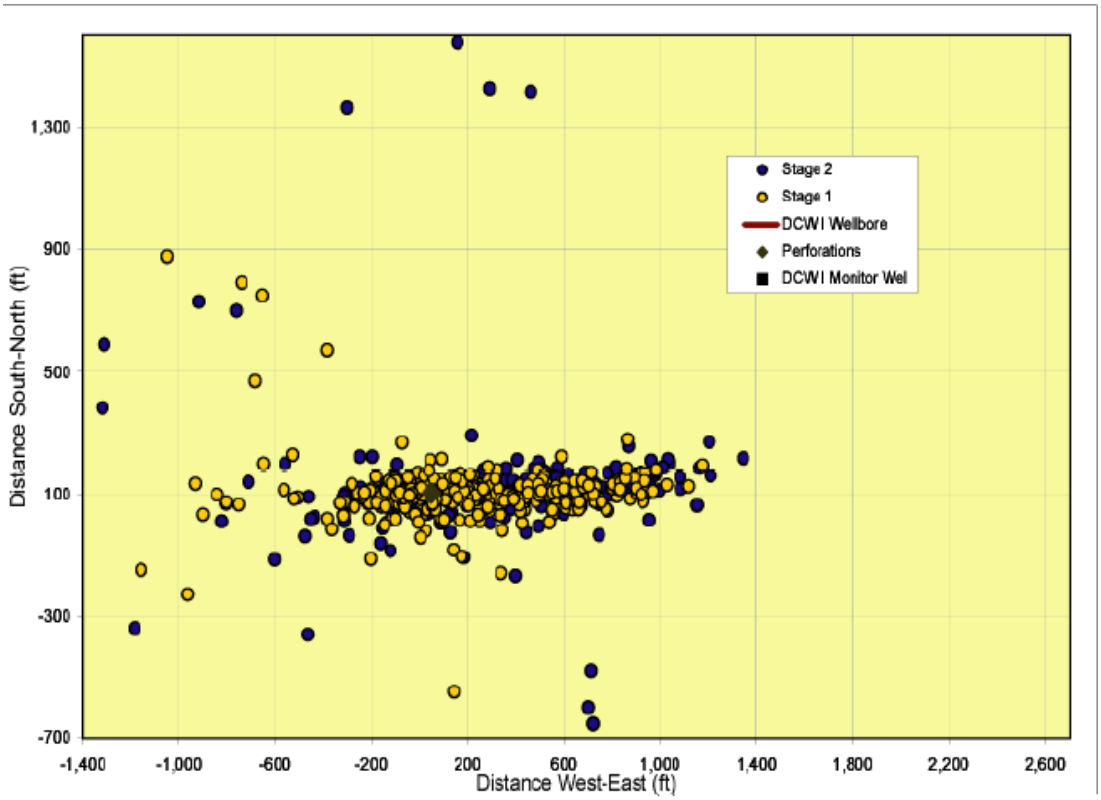

Figure 6 Map View of DCW I Microseismic Results for Both Stages

Table 1 DCW I Microseismic and Interpreted Results

Description	Stage 1 Microseismic Volume	Stage 1 Interpreted Geometry	Stage 2 Microseismic Volume	Stage 2 Interpreted Geometry
Azimuth	N87°E	N87°E	N87°E	N87°E
Total Length	2,348 ft	1,872 ft	2,651 ft.	1,909 ft
Length Along East Wing	1,175 ft	940 ft	1,346 ft	1,090 ft
Length Along West Wing	1,158 ft	932 ft	1,318 ft	819 ft
Top (TVD)	8,854 ft	8,925 ft	8,300 ft.	8,855 ft
Bottom (TVD)	9,868 ft	9,325 ft	10,347 ft.	9,070 ft
Height	1,014 ft	400 ft	2,047 ft.	215 ft

Hydraulic fracture modeling software was used to perform a pressure history match of the stage one treating pressure. **Figure 7** shows the hydraulic fracture profile

and proppant concentration after closure plot of the treating pressure history match with the microseismic results overlain. There is reasonably good agreement between the calibrated model results and the microseismic events.

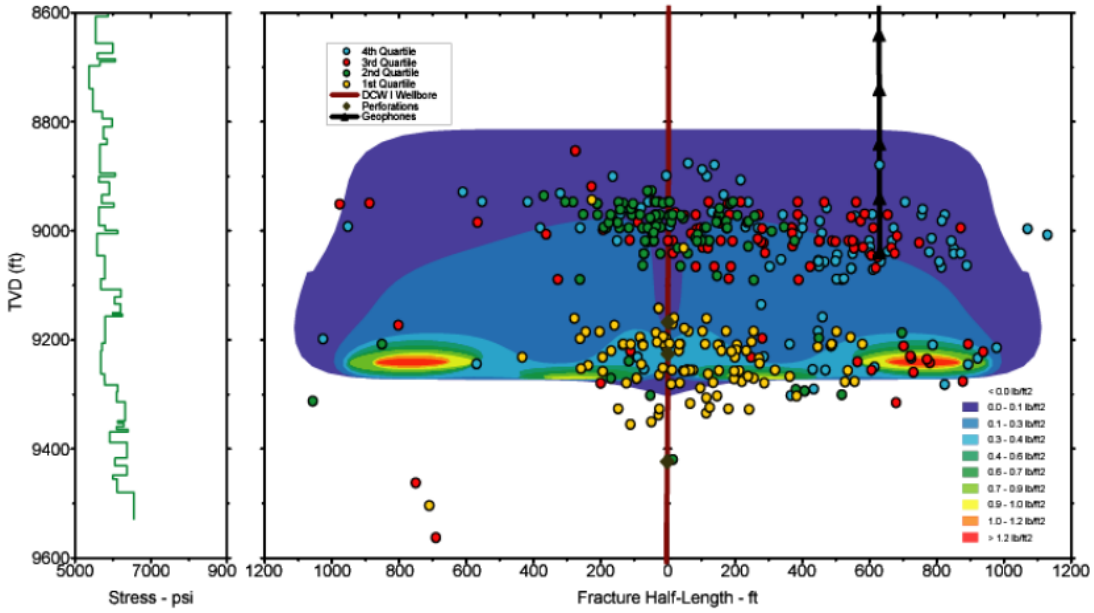

Figure 7 DCW I Stage One after Closure Proppant Concentration Plot with Microseismic Events

1.3 Objectives of Study

The followings are the objectives of study for this work:

- To develop a rigorous and innovative speed-up well performance model, based on DVS method, to calculate the dimensionless productivity index J_D for the horizontal well intercepted by multiple fractures

- To validate the results from rigorous simulator for well testing and production forecast by comparing the results with simple symmetric well and fracture configuration.
- To validate the applicability and demonstrate the advantage of the solution from speed-up simulator for the horizontal well intercepted by multiple fractures with the rigorous simulator
- To show the capability of the speed up production simulator to handle more complicated well/fracture configurations. Sensitivity study included well drainage size, asymmetry of the fracture wings, and curved well.
- To conduct field example studies using the production data and stimulation treatment data of gas wells from East Texas Cotton Valley.

CHAPTER II

METHODOLOGY

2.1 The Uniform Flux Solution for DVS Method

Consider an anisotropic and homogeneous medium without boundary flow, which stands for an ideal reservoir. There is a rectilinear source inside it, which presents the fracture schematic, with its surfaces parallel to the reservoir boundaries, which is showed in **Figure 8**.

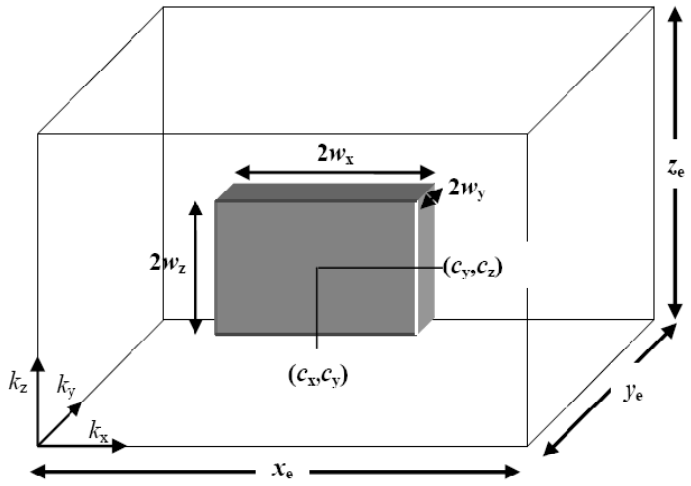

Figure 8 Frame Schematic of DVS Model

Begin with the original Green Function with an instantaneous source $\mathrm{Q(x,y,z,t)}$, which is distributed uniformly in the volume of the source, the diffusivity equation comes:

$$\eta_x \frac{\partial^2 p}{\partial x^2} + \eta_y \frac{\partial^2 p}{\partial y^2} + \eta_z \frac{\partial^2 p}{\partial z^2} + \frac{1}{\phi c_t} Q(x,y,z,t) = \frac{\partial p}{\partial t}$$

in which:

$$\eta_x = \frac{\mathrm{k_x}}{\phi\mu\mathrm{c}_t}$$

$$\eta_y = \frac{\mathrm{k_y}}{\phi\mu\mathrm{c}_t}$$

$$\eta_z = \frac{\mathrm{k_z}}{\phi\mu\mathrm{c}_t}$$

Initial Condition:

$$p(x, y, z, 0) = p_i$$

Boundary Condition:

$$\left.\frac{dp}{dx}\right|_{\mathrm{x=0}} = \left.\frac{dp}{dx}\right|_{\mathrm{x=x_e}} = 0$$

$$\left.\frac{dp}{dy}\right|_{\mathrm{y=0}} = \left.\frac{dp}{dy}\right|_{\mathrm{y=y_e}} = 0$$

$$\left.\frac{dp}{dz}\right|_{\mathrm{z=0}} = \left.\frac{dp}{dz}\right|_{\mathrm{x=z_e}} = 0$$

In order to simplify the calculation, we define the dimensionless variables as follow:

$$x_D = \frac{x}{x_e}$$

$$y_D = \frac{y}{y_e}$$

$$z_D = \frac{z}{z_e}$$

$$\mathrm{p_D} = \frac{\mathrm{kL}}{\mathrm{qB}\mu}(\mathrm{p_i} - \mathrm{p})$$

$$\mathrm{t_D} = \frac{\mathrm{k}}{\phi\mu\mathrm{c_t}\mathrm{L}^2}\mathrm{t}$$

We define k and L to be the reference permeability and reference length as follows:

$$\mathrm{k} = (\mathrm{k_x k_y k_z})^{\frac{1}{3}}$$

$$\mathrm{L} = (\mathrm{x_e y_e z_e})^{\frac{1}{3}}$$

We applied the method of separation of variables to solve the dimensionless Green Function with dimensionless boundary conditions.

From the Newman's principle, we describe the solution in 3D as the product of three 1D solutions with the source distributed along a finite section of the linear reservoir.

$$p_{\delta D}(box - pars; x_D, y_D, z_D, t_D)$$
$$= f(x - pars; x_D, t_{Dx}) \times f(y - pars; y_D, t_{Dy}) \times f(z - pars; z_D, t_{Dz})$$

In order to get pressure response correspond to a continuous unit source distributed uniformly in the box, we numerically integrate the $p_{\delta D}(x_D, y_D, z_D, \tau)$ over time:

$$p_{uD}(x_D, y_D, z_D, t_D) = \int_0^{t_D} p_{\delta D}(x_D, y_D, z_D, \tau) d\tau$$

(Valkó and Amini, 2007)

2.2 Pressure Response Related to Withdraw

We consider the finite conductivity condition. The pressure at each segment of the source is defined as the sum of the effect of the other segments:

$$\mathrm{P_{Di}} = \sum_{\mathrm{j=1}}^{\mathrm{n}} \mathrm{q_{Dj} p_{Di,j}}$$

$\mathrm{q_{Dj}}$represents the strength of the segment j, $\mathrm{p_{Di,j}}$ represents the dimensionless pressure calculated at the center of segment I as if the source is put in the segment j.

Figure 9 shows an example: the $p_{D1,6}$ is calculated by using the uniform flux solution for a continuous source, when dividing the source into 9 segments.

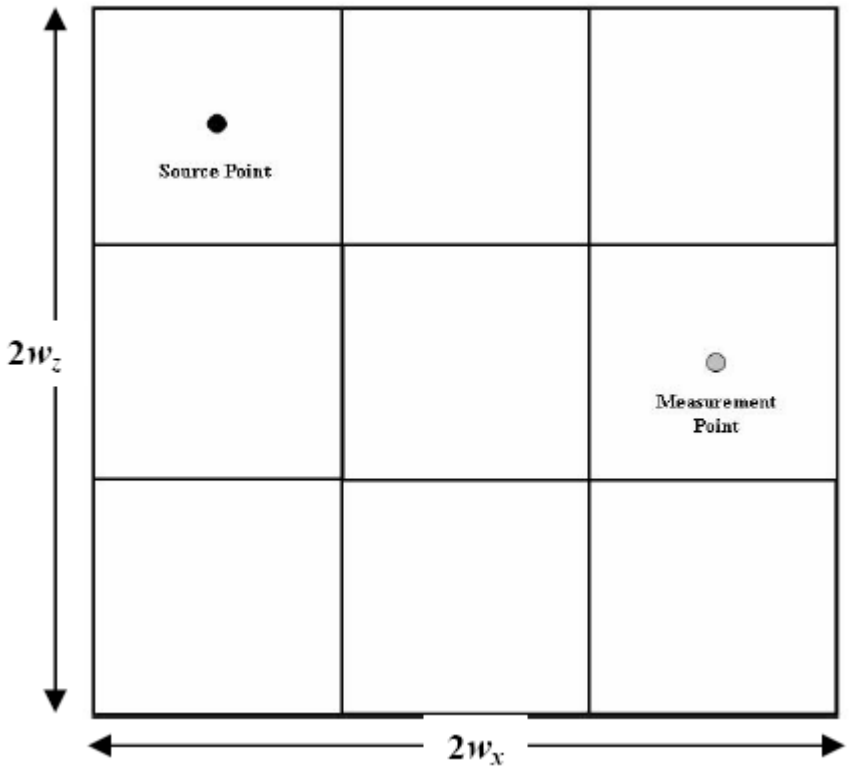

Figure 9 Calculation of $p_{D1,6}$ in 9 Segments Discretized Source

The matrix notation for the system is:

$$[\mathbf{A} + \mathbf{C}] \cdot \mathbf{q} - \mathbf{b} = \mathbf{0}$$

where

A is a (n × n) matrix containing $p_{Di,j}$ as its elements. The ij-th element of the "A" matrix is a function of the position of both boxes i and j in addition to the three dimensions of the j-th box. It represents the pressure response at the center of box i to an instantaneous withdrawal from the sub source j.

C is also a (n × n) matrix. The ij-th element describes the pressure drop in the fracture between the center of the i-th source and the wellbore reference point due to the j-th inflow. It is determined by the assumptions we make regarding the conductivity within the fracture.

q is the vector of strengths.

b is the vector with the elements all equal to wellbore flow pressure $p_{D,wf}$.

There are two cases of fluid flow inside the fracture we consider.

For the first case, the fluid flow in the source can be assumed 1D, for instance: a vertical well with vertically fully penetrated fracture (as showed in **Figure 10**) and horizontal well with longitudinal fracture.

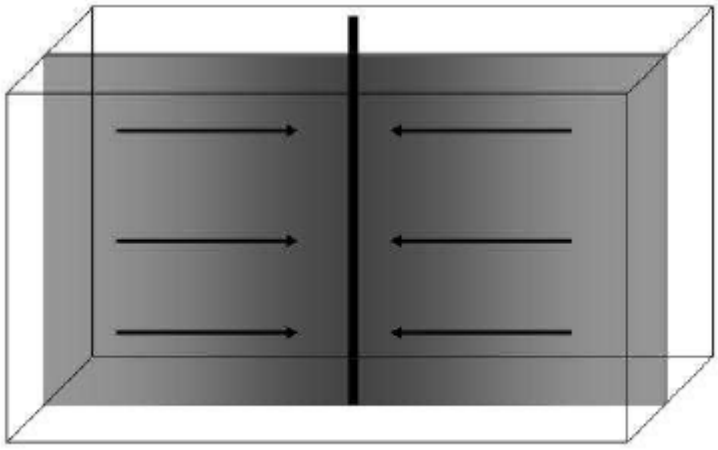

Figure 10 1D Flow in the Source

For example we discretize the source into 6 segments, locate the wellbore in the middle of the source (as shown in **Figure 11**).

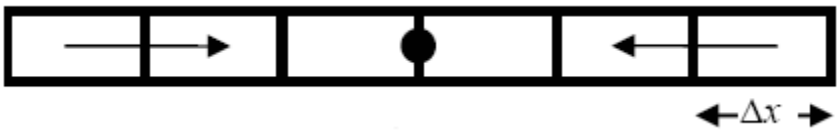

Figure 11 Schematic of a Discretized 1D Source

In this example, C matrix could be denotated to a coefficient matrix D times the variables:

$$C = \frac{2kLx_f}{4nw_y w_z k_f} D$$

The dimensionless coefficient matrix D for 6 linear segments here is:

$$D = \begin{bmatrix} \frac{19}{8} & \frac{3}{2} & \frac{1}{2} & & & \\ \frac{3}{2} & \frac{11}{8} & \frac{1}{2} & & 0 & \\ \frac{1}{2} & \frac{1}{2} & \frac{3}{8} & & & \\ & & & \frac{3}{8} & \frac{1}{2} & \frac{1}{2} \\ & 0 & & \frac{1}{2} & \frac{11}{8} & \frac{3}{2} \\ & & & \frac{1}{2} & \frac{3}{2} & \frac{19}{8} \end{bmatrix}$$

The zero elements mean the segments 4 to 6 do not contribute frictional pressure loss for the segments 1 to 3 to the wellbore.

For the second case, the fluid flow in the source can be assumed 2D, for instance: a vertical well with partially penetrated fracture (as showed in **Figure 12**) and horizontal well with transverse fracture.

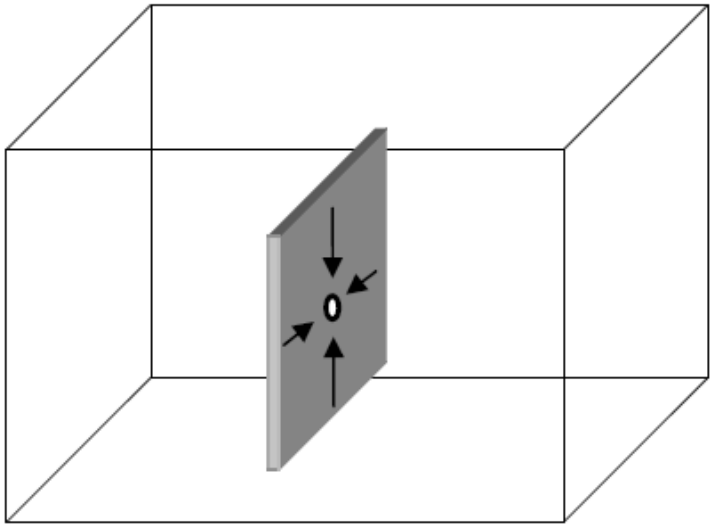

Figure 12 2D Flow in the Source

For the 2D flow inside fracture, here is a general finite different formulation in the steady state condition, which is a material balance equation containing Darcy's Law.

$$q_{i,j} = \frac{k_f 2 w_z}{\mu}\left[\frac{\Delta y}{\Delta x}\left(p_{i-1,j} + p_{i+1,j} - p_{i,j}\right) + \frac{\Delta x}{\Delta y}\left(p_{i,j-1} + p_{i,j+1} - p_{i,j}\right)\right]$$

in which $q_{i,j}$ represent the net production from the block (i,j). The schematic of a Discretized 2D Source and an example are shown in **Figure 13** and **Figure 14**.

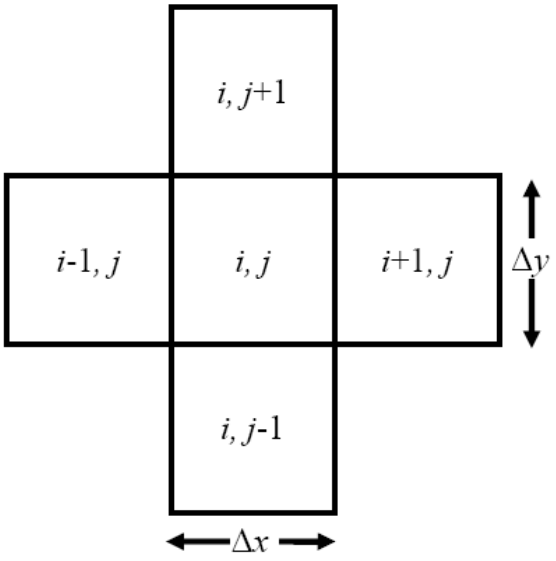

Figure 13 Schematic of a Discretized 2D Source

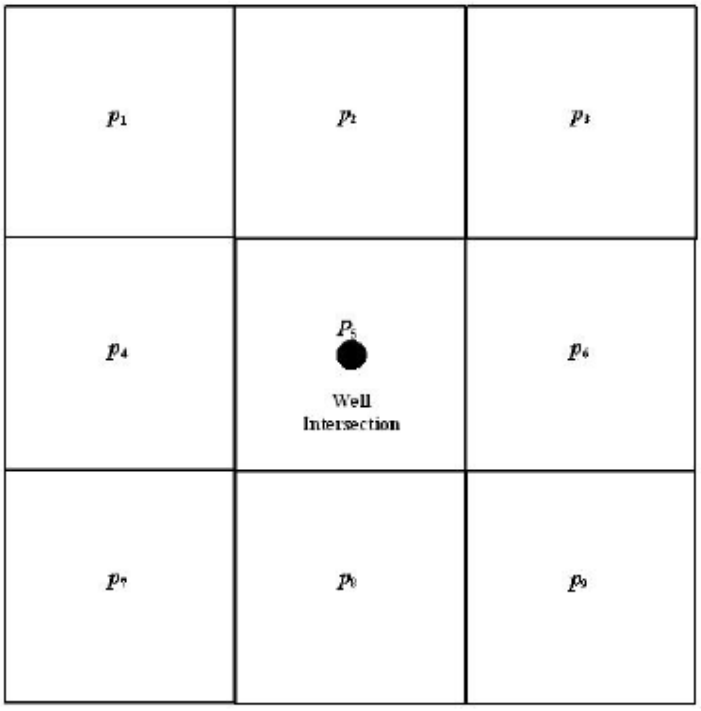

Figure 14 Example of a Discretized 2D Source

2.3 Relationship between Production Index and Pressure

The basic application in DVS method is to forecast production index for various well fracture configurations. From the production index, the production rate could be calculated easily, then we could have the cumulative production.

The productivity index is defined as the ability of the reservoir to produce hydrocarbon per unit pressure drop in the reservoir (volume/time/pressure).

$$J = \frac{q}{p_{avg} - p_{wf}}$$

in which

q = Flow Rate

p_{avg} = Average Reservoir Pressure

p_{wf} = Well Flowing Pressure

Introducing the Dimensionless parameters as the followings the expression for the Dimensionless productivity index would be obtained.

$$p_{D,trad} = \frac{2\pi kh}{qB\mu}(p_i - p)$$

$$J_D = \frac{\mu B}{2\pi kh} J$$

with:

p_i = Initial Reservoir Pressure

k = Reservoir Permeability

h = Reservoir Thickness

B = Formation Volume Factor

μ = Fluid Viscosity

Combining the three equations above we have:

$$J_D = \frac{1}{p_{D,trad} - p_{D,avg,trad}}$$

Assuming a constant and small compressibility during depletion we can write:

$$c_t = -\frac{1}{V}\frac{\partial V}{\partial p}$$

$$V = \phi Ah$$

$$\frac{\partial p}{\partial V} = \frac{1}{\phi Ahc_t}$$

$$\Delta p = p_i - p_{avg} = \frac{\Delta V}{\phi Ahc_t} = \frac{N_p B}{\phi Ahc_t} = \frac{qBt}{\phi Ahc_t} \text{ (Constant flow rate production)}$$

Using the definition for dimensionless pressure and applying it on the equation above, we have:

$$p_{D,avg,trad} = 2\pi \frac{kt}{\phi\mu c_t A} = 2\pi t_{DA}$$

where:

$$t_{DA} = \frac{kt}{\phi\mu c_t A} \text{ (Dimensionless time defined based on drainage area)}$$

When the reservoir is rectilinear with both length L

$$\mathrm{t_D} = \frac{\mathrm{k}}{\emptyset \mu \mathrm{c_t L^2}} \mathrm{t} \text{ (Another way to define dimensionless time)}$$

$$t_{DA} = c_{trad}\, t_D$$

We are leaded to an expression correlating the dimensionless productivity index as a function of dimensionless pressure and dimensionless time, which shown below.

$$J_D = \frac{1}{2\pi c_{trad}(p_{uD} - t_D)}$$

Or

$$J_D = \frac{1}{p_{D,trad} - 2\pi t_{DA}}$$

where,

$$c_{trad} = \frac{z_e \sqrt{k_x k_x}}{L k}$$

$$p_{uD} = \int_0^{t_D} p_{\delta D}(t_D^{'}).dt_D^{'}$$

In field units, the productivity index is expressed as

$$PI = \frac{z_e \sqrt{k_x k_y}}{141.2 B \mu} J_{D,trad}$$

The main task of DVS is first to predict the pressure behavior of well fracture configurations; And then take use of the pressure data to predict the productivity index (PI) behavior – the productivity index in especially pseudosteady state is a measurement of producing capability from the reservoir; At last, when comparing the pseudosteady state productivity index in different completion schemes, evaluate which scheme performs most efficiently. (Amini, 2007)

CHAPTER III

APPLICATION OF DVS METHOD IN GAS PRODUCTION FORECASTING

3.1 Introduction

This work solves the problem of production forecasting of transient and pseudo-steady-state production from a horizontal well intercepted by multiple vertical fractures in a rectilinear reservoir with closed boundaries. **Figure 15** shows the start-up screen, which offers 5 "tabs": Input, Calculate JD, Results, Show state and Help. To work with this program, first click "Input". In the second row of tabs the following options can be seen: Reservoir properties, Gas properties, Adsorption properties and Source properties. Go through all these tabs, one by one (Valkó, 2008). In the third row of tabs, there are eight options can be seen, which allow users to choose the number of fracture stages. The graphical interface shows horizontal well with five finite conductivity vertical fracture – intersecting the well transversely. The input screen allows moving the well in the reservoir and the fracture along and transverse the well, in addition to sizing the fracture and changing the permeability inside the fracture. The wellbore radius is also an input variable under the "one fracture" tab.

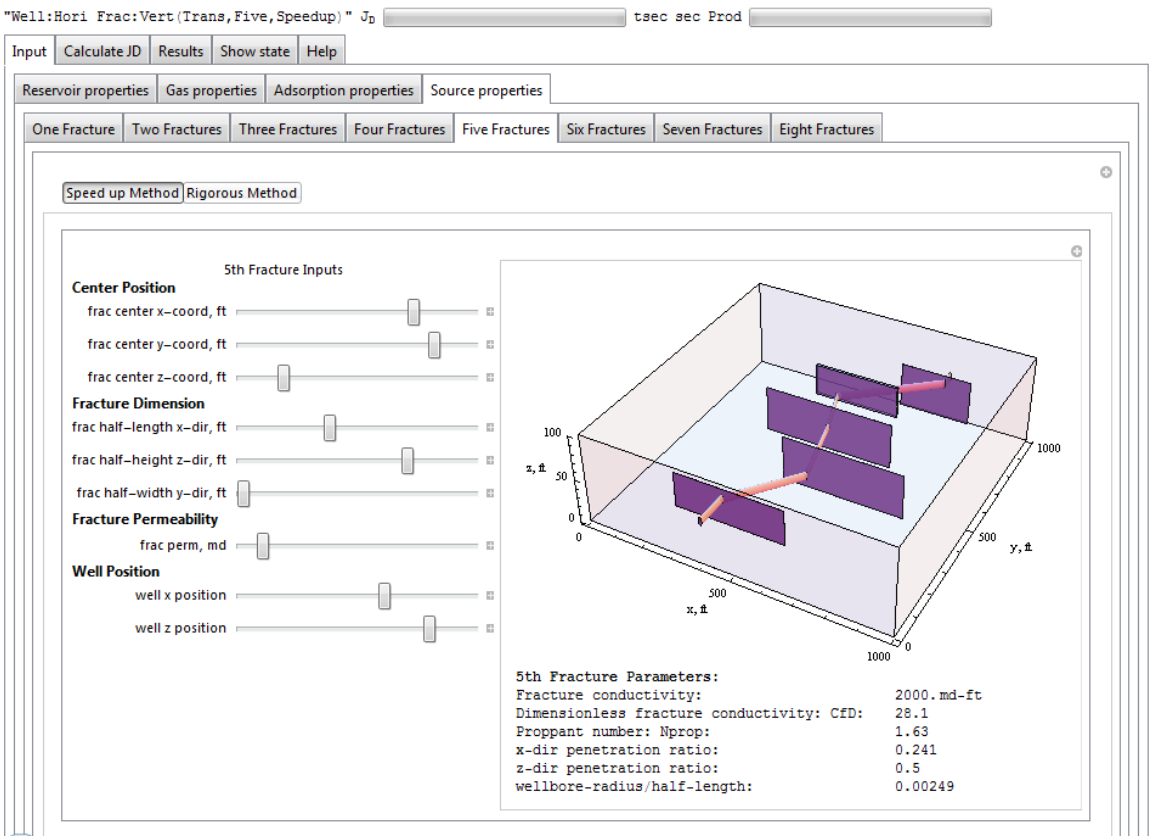

Figure 15 Schematic of the Software Interface

3.2 Rigorous Productivity Index Forecasting Method for Multiple Fractures Model

The first step of our work is to develop a rigorous method to calculate the dimensionless productivity index J_D for such well-fracture configurations.

According to the method of Distributed Volumetric Sources (DVS), a single finite conductivity fracture intersected by a well is modeled as follows:

We divide the fracture into several grids, e.g. 4 or 8. Then we write the governing equations in matrix notation to determine the strength of each box:

$$[\mathbf{A} + \mathbf{C}] \cdot \mathbf{q} - \mathbf{b} = \mathbf{0}$$

The ij-th element of the **A** matrix is a function of the position of both boxes i and j in addition to the three dimensions of the j-th box. It represents the pressure response at the center of box i to an instantaneous withdrawal from the sub source j.

The **C** matrix stands for the pressure losses due to the finite conductivity along the path of the fluid from box I to the wellbore reference point. It is determined by the assumptions we make regarding the conductivity within the fracture.

q is the vector of strengths.

b is the vector with the elements all equal to wellbore flow pressure $p_{D,wf}$.

To model multiple transverse fractures in the DVS framework, each fracture would be divided into boxes and **A** matrix is constructed by calculating the pressure response reacting to the withdrawal from each sub-source, within the same fracture and within all the other fractures. At the same time, we extend the **C** matrix to indicate the pressure losses from the center of each box to the reference point in the wellbore.

Couples of examples in different fluid flow cases are given to illustrate how to solve multiple fractures problem by taking use of the DVS method.

In the first case, the fluid flow in the source is assumed one dimension. The wellbore located in the center of the source, and the source could be discretized into segments, along the direction of the propagation of the fracture, as shown in **Figure 16**.

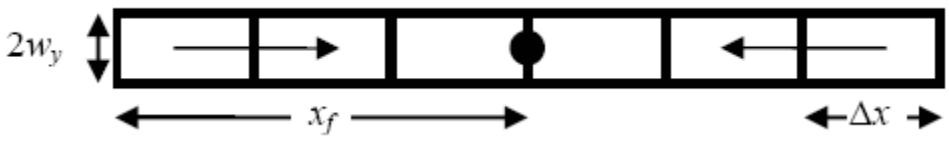

Figure 16 Schematic of a Discretized 1D Fluid Flow inside Fracture

The example shows the well performance forecasting, in a regular permeability rectilinear reservoir with closed outer boundaries, with reservoir drainage area and net pay 1000ft*1000ft, 180ft, respectively. Inside the reservoir, three identical parallel transverse fractures are intersected along a horizontal well. As showed in **Figure 17**, each fracture is divided into 8 segments, and the fluid flow goes from the reservoir to the wellbore along the arrow in Figure 17. The input reservoir and fracture parameters are summarized as shown in **Table 2**.

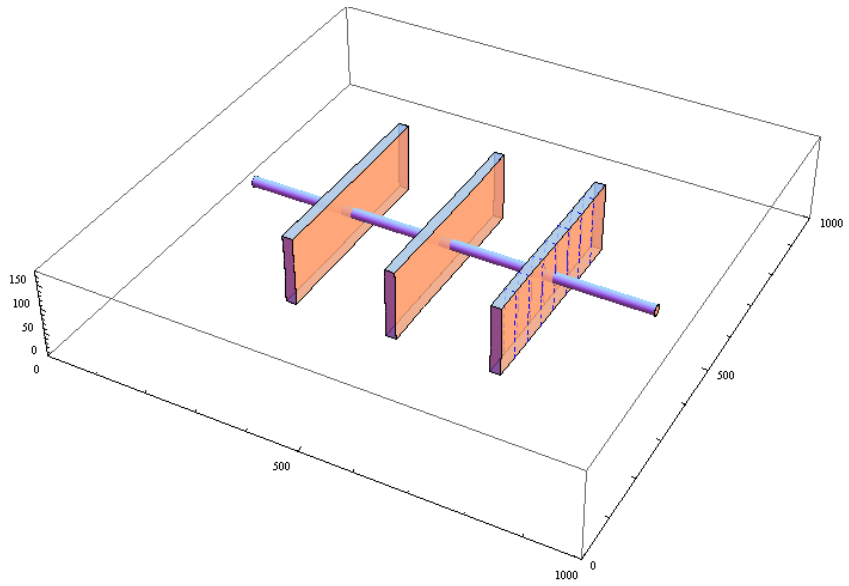

Figure 17 1 Dimension Fluid Flow Schematics of Three Transverse Fractures Intersected by a Horizontal Well

Table 2 Summary of Input Parameters for Horizontal Well with Three Transverse Fractures, Reservoir and Fracture Parameter (1D Flow)

Reservoir parameters	Fracture No1 parameters	Fracture No2 parameters	Fracture No3 parameters
x_e = 1000 ft	Center location:	Center location:	Center location:
y_e = 1000 ft	Cx=500 ft	Cx=500 ft	Cx=500 ft
z_e = 180 ft	Cy=300 ft	Cy=500 ft	Cy=700 ft
k_x = 3 md	Cz=90 ft	Cz=90 ft	Cz=90 ft
k_y = 3 md			
k_z = 3 md	Half length:	Half length:	Half length:
	w_x= 200 ft	w_x= 200 ft	w_x= 200 ft
	w_y=0.3 ft	w_y=0.3 ft	w_y=0.3 ft
	w_z=70 ft	w_z=70 ft	w_z=70 ft
	Fracture permeability:	Fracture permeability:	Fracture permeability:
	k_{fx}=60000 md	k_{fx}=60000 md	k_{fx}=60000 md

With these input parameters, the productivity index is calculated by multiple fractures DVS program. The obtained dimensionless productivity index as a function of dimensionless time t_D is shown in **Figure 18**. The productivity index is a parameter to measure the reservoir and well performance. An optimum fracture design and completion scheme result from the productivity index information.

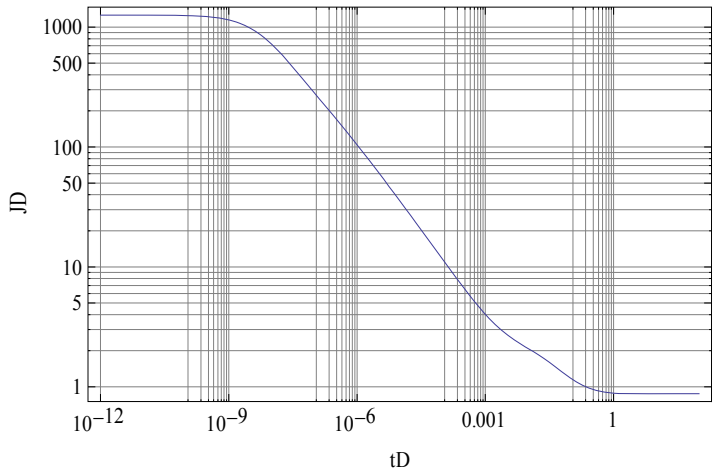

Figure 18 Plot of Calculated Dimensionless Productivity Index Forecast for Three Fractures Intersected by a Horizontal Well

In the other case, the fluid flow in the source is assumed to be two dimensions. The wellbore located in the center of the source, and the source could be discretized into segments, along the height and length direction of the fracture, as shown in **Figure 19**.

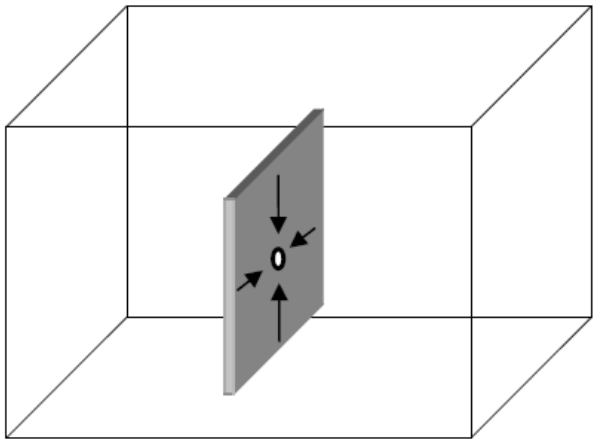

Figure 19 2D Flow in the Source

The second example shows the well performance forecasting, in a low permeability rectilinear reservoir with closed outer boundaries, with reservoir drainage area and net pay 1000ft*1000ft, 180ft, respectively. Inside the reservoir, three identical parallel transverse fractures are intersected along a horizontal well, which is showed in **Figure 20**. As showed in Figure 20, each fracture is divided into 9 segments, and the fluid flow goes from the reservoir to the wellbore along the arrow in Figure 19. The input reservoir and fracture parameters are summarized as shown in **Table 3**.

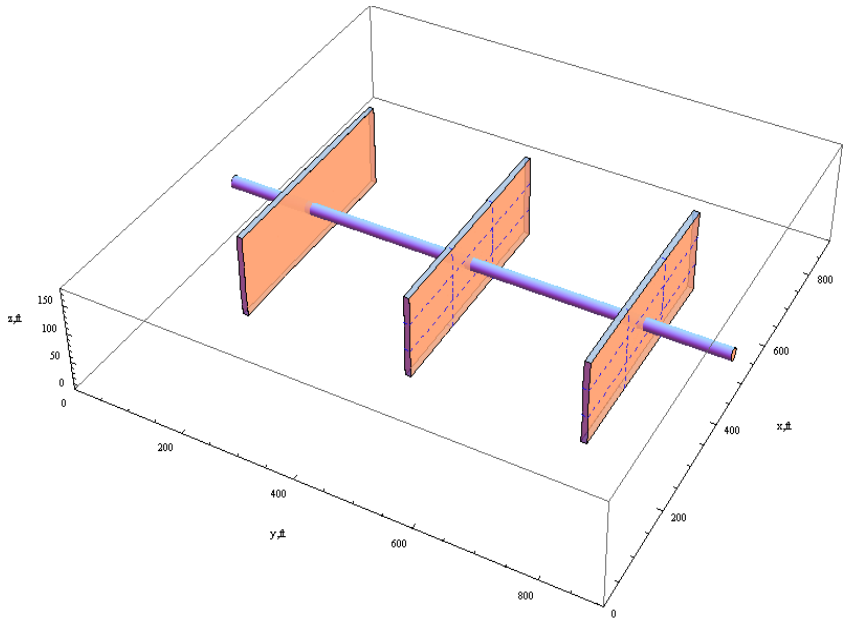

Figure 20 2 Dimensions Fluid Flow Schematics of Three Transverse Fractures Intersected by a Horizontal Well

Table 3 Summary of Input Parameters for Horizontal Well with Three Transverse Fractures, Reservoir and Fracture Parameter (2D Flow)

Reservoir parameters	Fracture No1 parameters	Fracture No2 parameters	Fracture No3 parameters
x_e = 1000 ft y_e = 1000 ft z_e = 180 ft k_x = 0.1 md k_y = 0.1 md k_z = 0.05 md	Center location: Cx=500 ft Cy=300 ft Cz=90 ft Half length: w_x= 200 ft w_y=0.3 ft w_z=70 ft Fracture permeability: k_{fx}=60000 md	Center location: Cx=500 ft Cy=500 ft Cz=90 ft Half length: w_x= 200 ft w_y=0.3 ft w_z=70 ft Fracture permeability: k_{fx}=60000 md	Center location: Cx=500 ft Cy=700 ft Cz=90 ft Half length: w_x= 200 ft w_y=0.3 ft w_z=70 ft Fracture permeability: k_{fx}=60000 md

With these input parameters, in accordance with each sub-sources, calculate the pressure interaction between each sub-source, as well as the pressure losses due to finite conductivity along the path of the fluid in the fracture, the productivity index is finally calculated by multiple fractures DVS program. The obtained dimensionless productivity index as a function of dimensionless time t_D is shown in **Figure 21**. The productivity

index is a parameter to measure the reservoir and well performance. The 2 dimensions fluid flow model, shown in Figure 19, makes more reasonable, than 1 dimension fluid flow model, shown in Figure 16, in the case of transverse fracture, and obtain more accurate results in the multiple transverse fractures intersected by horizontal well. The 2D fluid flow model will be used in the rest of the research work.

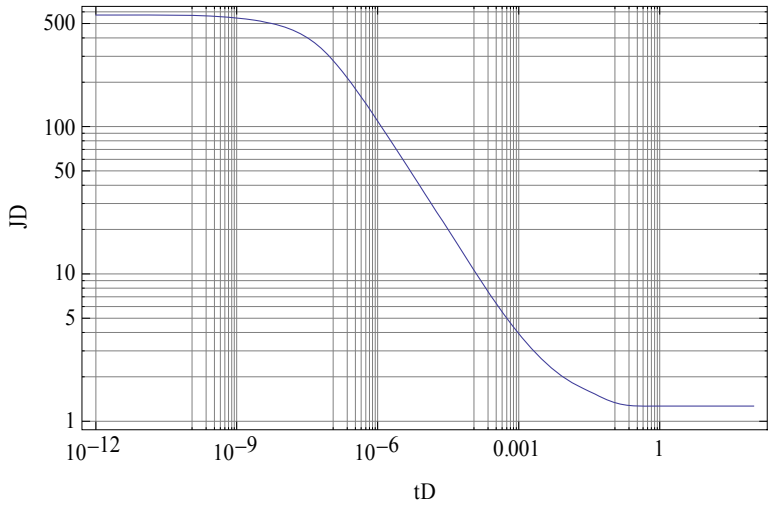

Figure 21 Plot of Calculated Dimensionless Productivity Index Forecast for Three Fractures Intersected by a Horizontal Well (2D Flow)

This section presents a straightforward generalization of the DVS method. We call it the "rigorous" approach, for it gives the most accurate results, and does not contain any additional simplification. As expected, the rigorous method is computationally demanding.

3.3 Verify the Rigorous Method

So far, the rigorous multiple transverse fracture DVS method has been established to forecast the productivity index. By taking use of the pressure difference, production rate is calculated from the productivity index. As long as we have the production rate verse each time period, a comparison of two different simple cases will be shown to demonstrate the liability of this rigorous method.

First case shows a normal rectilinear reservoir containing three identical fractures, which is the same example in **Figure 20**. **Figure 22** plots the production rate according to each time within 200 days.

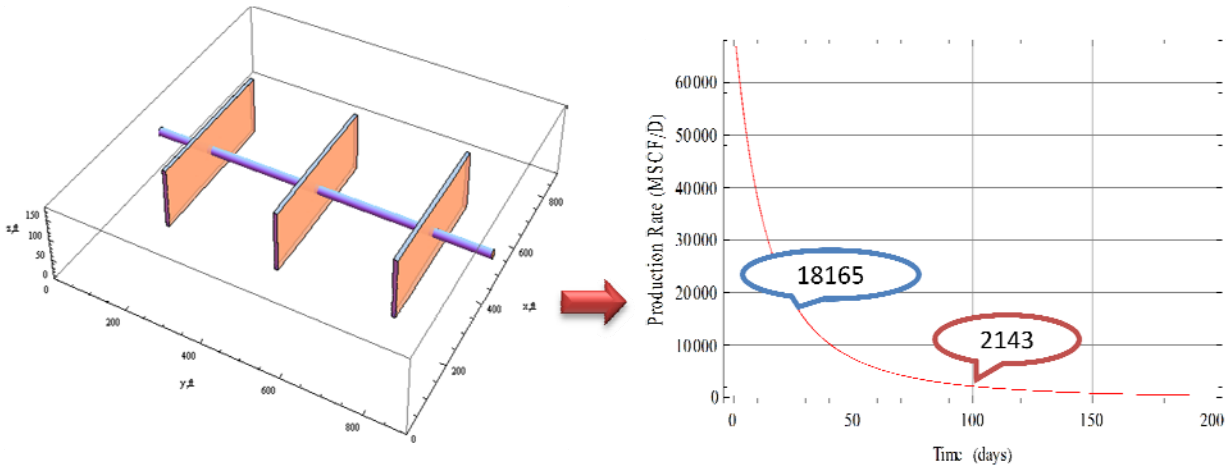

Figure 22 Production Data for Three Transverse Fractures in One Reservoir Configuration

The second case uses the same size reservoir with the same property. All the fractures are exactly in the same position, with the same parameters. The whole reservoir was assumed to be divided into three small segment reservoir; then each fracture is

located in the center of the reservoir. Because the three divided reservoir are symmetric, there is no fluid flow through any boundary between the reservoirs. We use the no flow boundary basic DVS method to forecast the production rate individually for each divided reservoir, and add them together, which is presented in **Figure 23**.

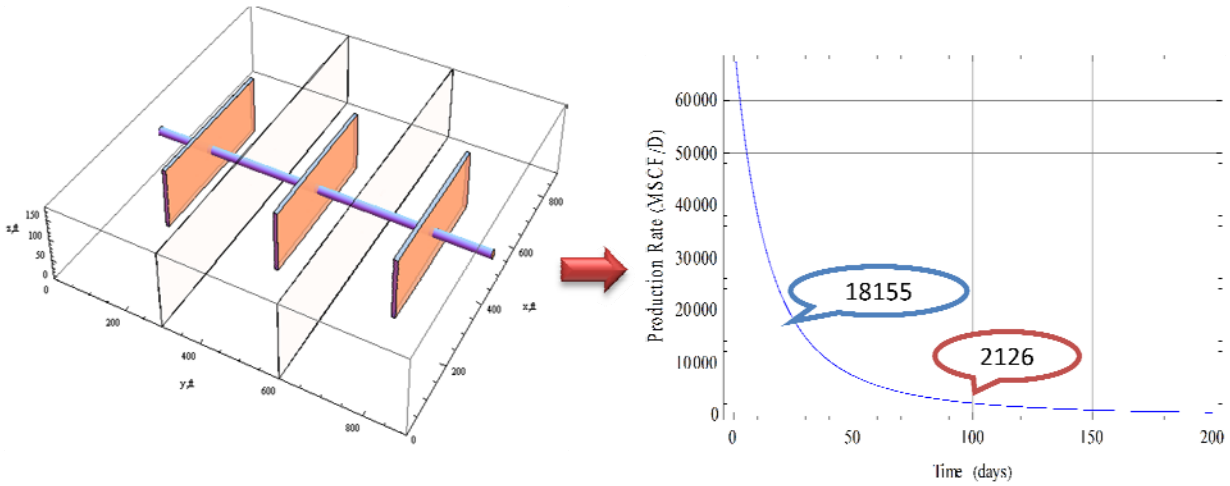

Figure 23 Production Data for Tansverse Fracture in Three Isolated Reservoir Configuration

The total production from the three divided reservoirs is supposed to be the same as the production from the system shown in **Figure 22**.

A comparison is conducted below. In an easily visible way, two production rate data is picked up from **Figure 22** and **Figure 23**, separately.

For the first case, 18165 MSCF/D on the 30th day production, 2143 MSCF/D on the 100th day production; for the second divided reservoir case, 18155 MSCF/D on the

30th day production, 2126 MSCF/D on the 100th day production. The error is calculated as follows:

$$\frac{18165 - 18155}{18155} = 0.05\%$$

$$\frac{2143 - 2126}{2126} = 0.8\%$$

The error is restricted within one percent, from the two target point comparison.

By tying the two curves into one graph, we cannot differentiate between them, by our bare eyes, as showed in **Figure 24**. Then, a more completed error analysis is conducted.

$$Error = \left|\frac{q1 - q2}{q2}\right| \times 100\%$$

Percentage of production rate difference divided by the reference production rate is used to show the error range in **Figure 25**. The result presents the error of the rigorous method is confined within 2%, which stands a good agreement with results from the original DVS method.

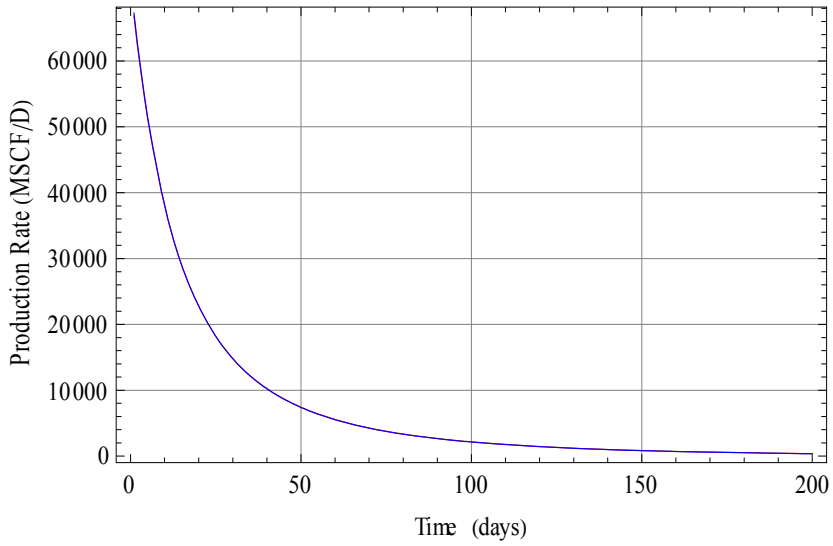

Figure 24 Comparison of Production Data for Transverse Fracture in Three Isolated Reservoir Configuration

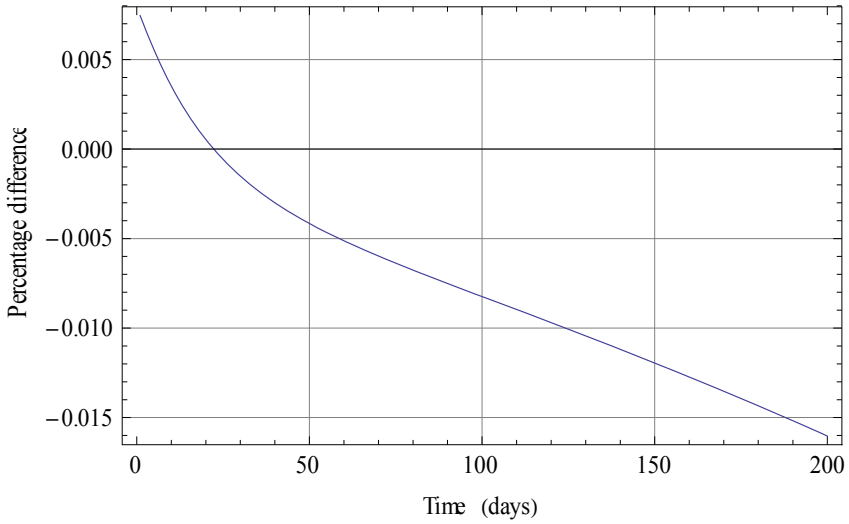

Figure 25 Error Analysis of Production Data for Transverse Fracture in Three Isolated Reservoir Configuration

3.4 Improved Productivity Index Forecasting Method for Multiple Fractures (Speedup Method)

So far, the box-in-box model in DVS method has been used to directly solve the problem of multiple fractures intercepted by a horizontal well in the rigorous method. The advantage of this rigorous method is obtaining accurate and reliable results, yet taking much computational time, when used to deal with a great mount of parallel fractures.

In the following, we investigate the possibility to reduce the computational time for such a complex well fracture model without compromising accuracy. The foundation of DVS theory is expressed in:

$$[\mathbf{A}+\mathbf{C}]\cdot\mathbf{q}-\mathbf{b}=\mathbf{0}$$

The most time consuming part of the DVS method is the calculation of the elements of the "A" matrix. The "A" matrix has $(n_0 \times n)^2$ elements, where n denotes the number of fractures along the horizontal well, and n_0 represents the number of volumetric sources within one fracture.

As a simple example, we consider 5 fractures along a horizontal well and divide each fracture into 8 boxes. In this case, "A" is a 40*40 matrix; therefore, we have to calculate 1600 elements of the "A" matrix.

In order to reduce the necessary computational time, we approximate certain elements of the "A" matrix by a fast calculation method. The basic idea is to retain the rigorous calculation for each element representing an interaction of two boxes within one fracture, for example the interaction denoted "1" in **Figure 26**, but to substitute the elements representing interaction between boxes in different fractures, for instance the

interaction denoted “2” in **Figure 26**, with the effect of two whole fractures, taking the center point as the reference point. After the simplification, we calculate the productivity index in a considerably short time. **Figure 27** shows the plot of productivity index vs. dimensionless time curve.

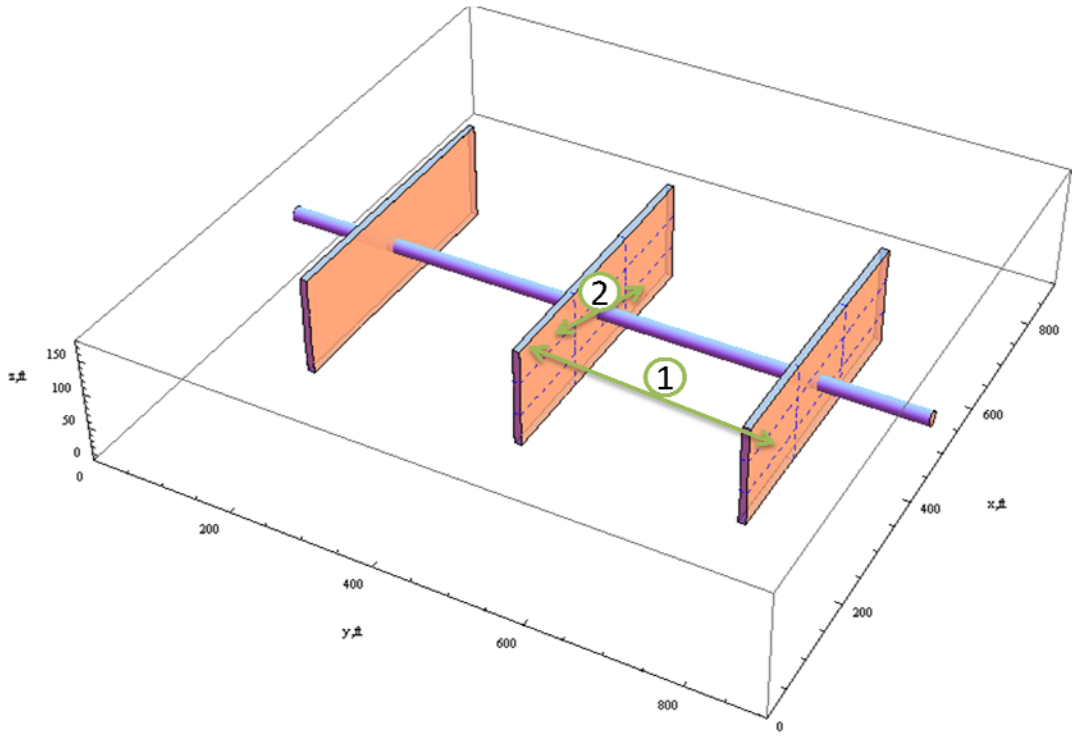

Figure 26 Schematic of Interaction between Fracture and within Fracture

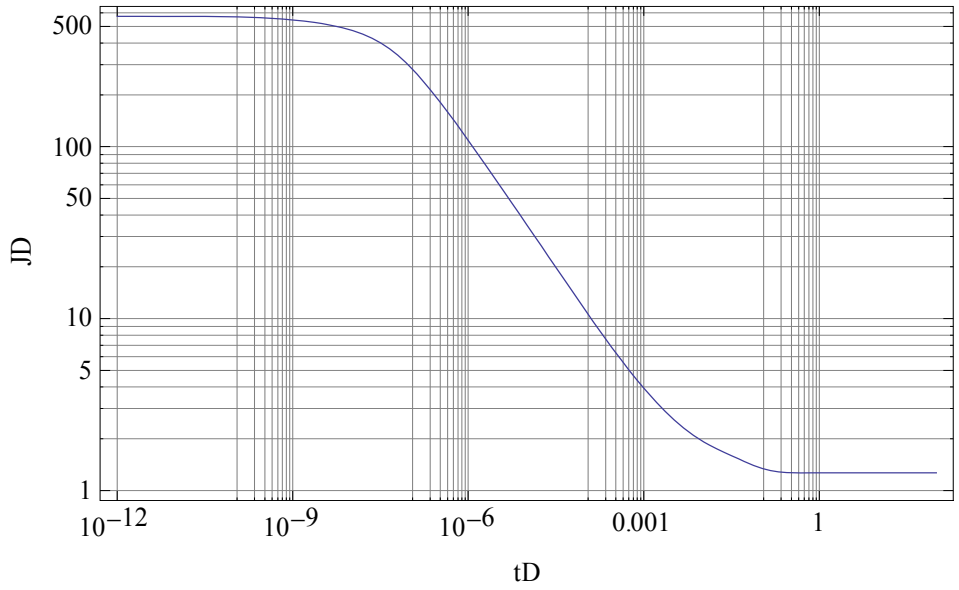

Figure 27 Speedup Calculated Dimensionless Productivity Index Forecast for Three Fractures Intersected by a Horizontal Well

3.5 Validation of the Speeding up Method

Based on the reservoir and fracture input parameters as shown in **Table 2**, a result comparison is conducted between speedup method and rigorous method. For the configuration of three transverse fractures intersected by a horizontal well, **Figure 28** shows the productivity index calculated by rigorous method; **Figure 29** shows the productivity index calculated by speedup method.

In **Figure 30**, two productivity index curves are placed together. For the case of three fractures, each with half length 200 ft, and the distance between them also 200 ft, the speed up method curve cannot be differentiated from the rigorous method curve with the naked eye, expect the end of the two curves.

From the picked out points in the two curves, the error is shown below:

$$\frac{1.26895-1.25901}{1.26895}=0.78\%$$

In order to figure out the error range, a percentage of difference is conducted to show in **Figure 31**. From the error test, at the end of two curves, the agreement stands with an error less than 1%, thus, an excellent agreement is found between the results of the two different methods presented.

Therefore, our goal right now is to determine the condition for the applicability of the speedup method which is clearly less demanding regarding computation time. The results from a mount of example tests are: there is a good agreement in the productivity index, as long as the distance between two neighboring fractures is larger than the half-length of the fracture.

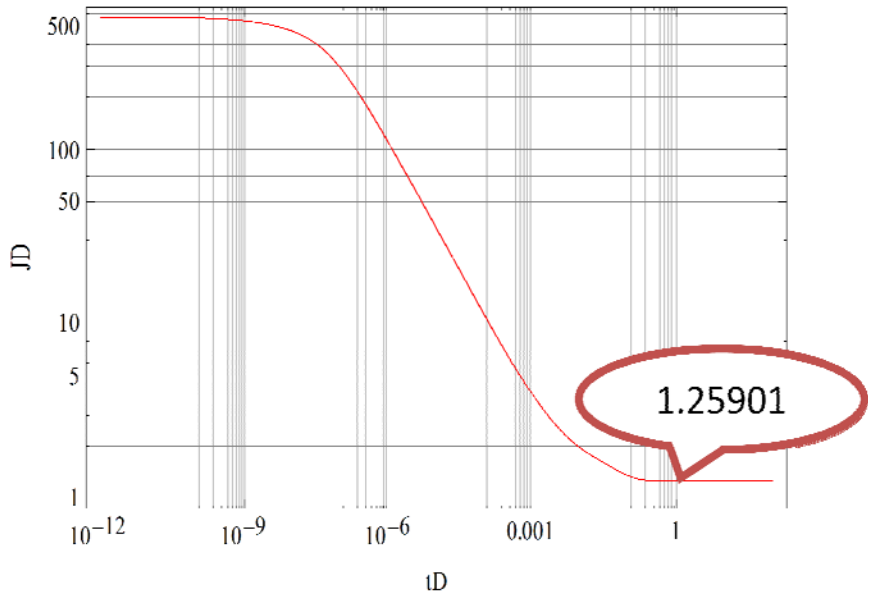

Figure 28 Dimensionless Productivity Index Calculated from Rigorous Method in the Configuration of Three Fractures Intersected by a Horizontal Well

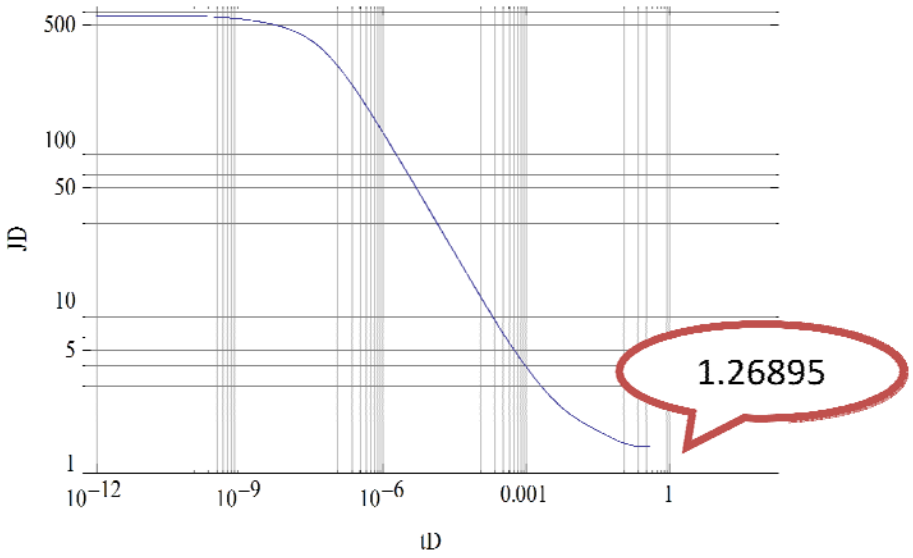

Figure 29 Dimensionless Productivity Index Calculated from Speedup Method in the Configuration of Three Fractures Intersected by a Horizontal Well

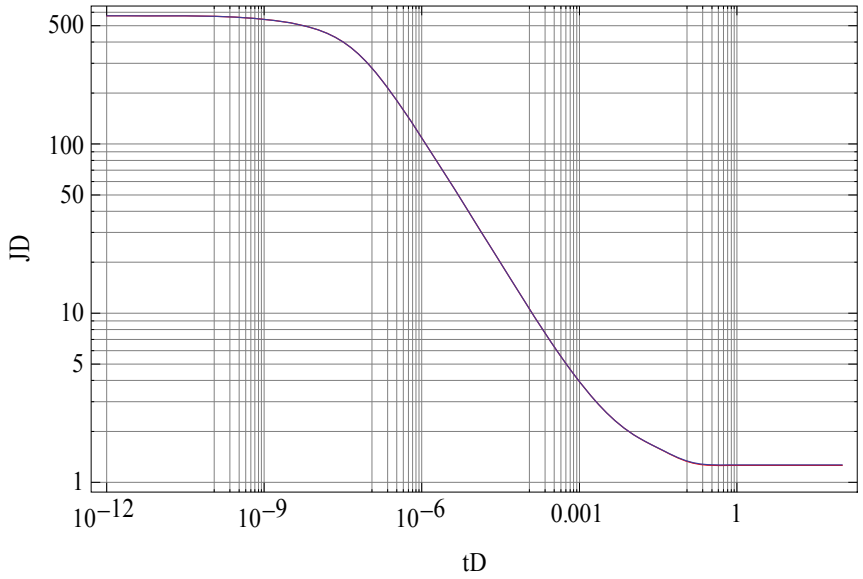

Figure 30 Comparison of Speedup Method Results with Rigorous Method for Dimensionless Productivity Index Forecasting of Three Fractures Intersected by a Horizontal Well

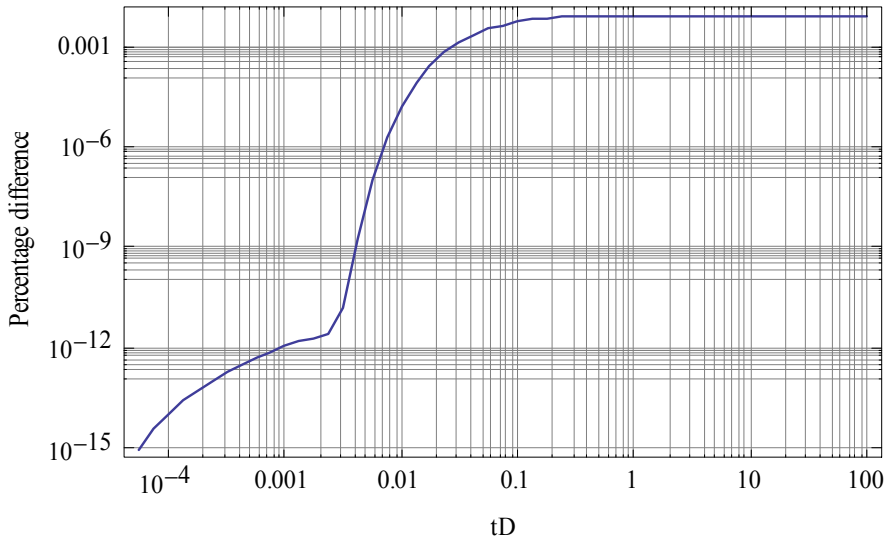

Figure 31 Percentage of Difference between Speedup Method and Rigorous Method for Dimensionless Productivity Index Forecasting of Three Fractures Intersected by a Horizontal Well

3.6 Advantage of Speedup Method

As stated above, speedup method is supposed to reduce the computational time, compared to rigorous method. A much more in details computational time comparison will be provided below to demonstrate the advantage of the speedup method, especially as the number of fractures grows.

One dimension fluid flow case: For the configuration of three transverse fractures intersected by a horizontal well, shown in **Figure 32**, computational time is tested for a various number of segments divided inside the fracture, such as 8 segments, 16 segments, and 32 segments. The time saved ratio results are around 2.2, which is shown in **Table 4**.

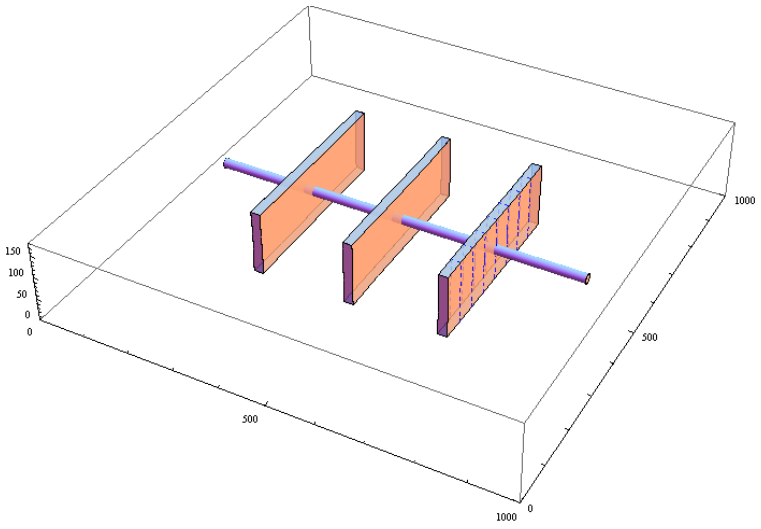

Figure 32 1 Dimension Fluid Flow Schematics of Three Transverse Fractures Intersected by a Horizontal Well

Table 4 Time Consumption Comparison for 3 Fractures Case in 1 Dimension Fluid Flow Schematics

Number of Box in Each Fracture, n	Time spent for rigorous method	Time spent for modified method	Saved Time Ratio
8	1.88	0.89	2.11
16	7.14	3.17	2.26
32	27.91	12.36	2.26

For the configuration of five transverse fractures intersected by a horizontal well, shown in **Figure 33**, time consumptions are tested for a various number of segments divided inside the fracture, such as 4 segments, 8 segments, and 16 segments. The time

saved ratio results are around 3.2, which is concluded in **Table 5**. The advantage of the speedup method becomes more evident, as the number of fractures increases.

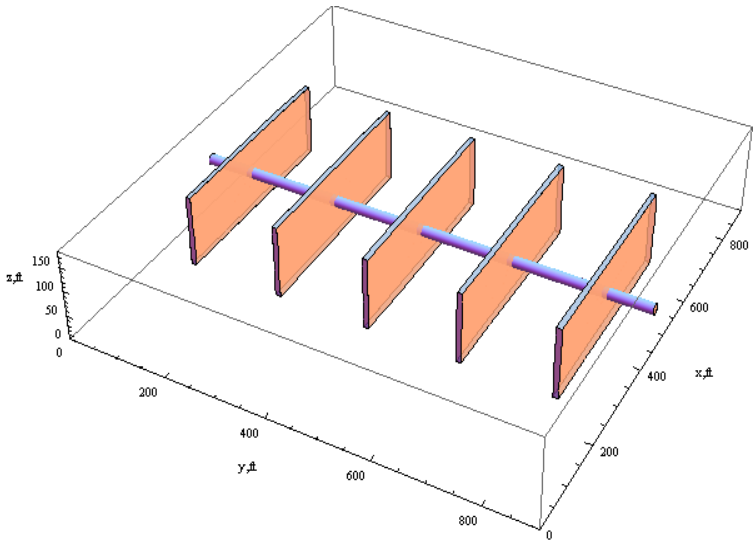

Figure 33 1 Dimension Fluid Flow Schematics of Five Transverse Fractures Intersected by a Horizontal Well

Table 5 Time Consumption Comparison for 5 Fractures Case in 1 Dimension Fluid Flow Schematics

Number of Box in Each Fracture, n	Time spent for rigorous method	Time spent for modified method	Saved Time Ratio
4	1.32	0.53	2.50
8	5.00	1.53	3.25
16	18.47	5.29	3.49

Two dimensions fluid flow case: For the configuration of three transverse fractures intersected by a horizontal well, shown in **Figure 34**, time consumptions are tested for a various number of segments divided inside the fracture, such as 9 segments, and 25 segments. The time saved ratio results are around 2.47, which is concluded in **Table 6**.

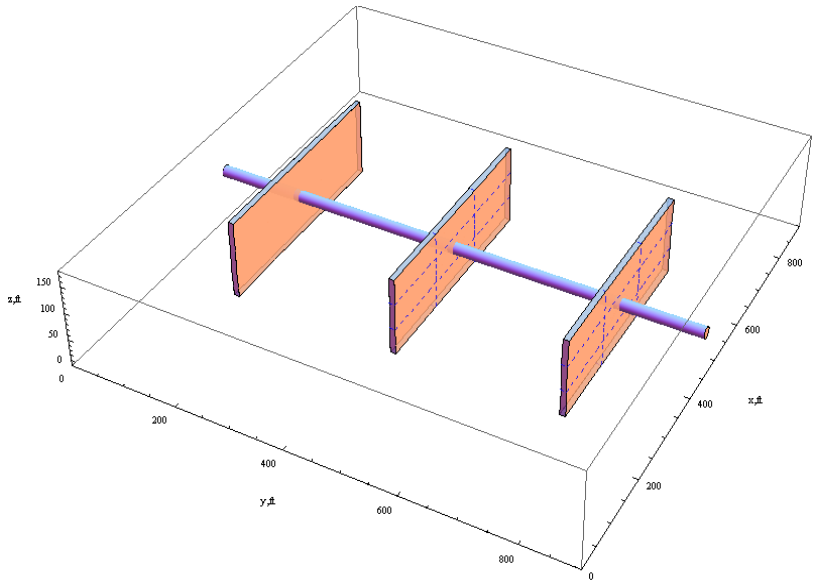

Figure 34 2 Dimensions Fluid Flow Schematics of Three Transverse Fractures Intersected by a Horizontal Well

Table 6 Time Consumption Comparison for 3 Fractures Case in 2 Dimensions Fluid Flow Schematics

Sub-Source Number	**Rigorous Method (min)**	**Speed up Method (min)**	**Speed up Ratio**
nx=1, nz=1 N=9	1.61	0.65	2.48
nx=2, nz=2 N=25	11.3	4.58	2.47

For the configuration of five transverse fractures intersected by a horizontal well, shown in **Figure 35**, time consumptions are tested for a various number of segments divided inside the fracture, such as 9 segments, and 25 segments. The time saved ratio results are around 3.5, which is concluded in **Table 7**.

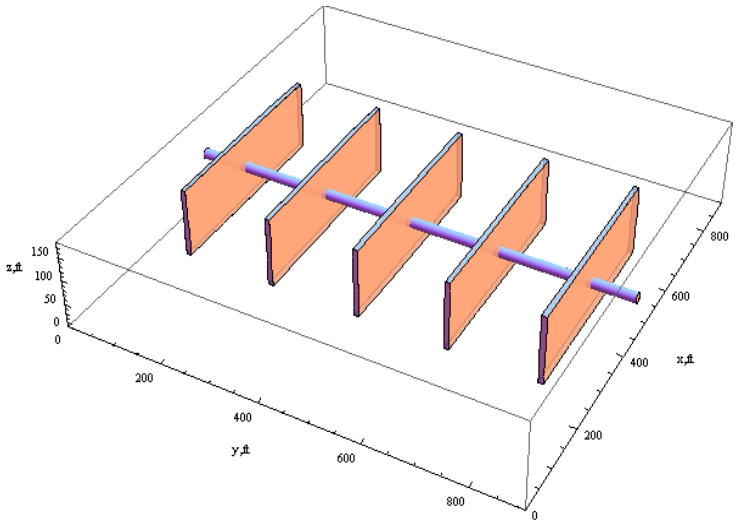

Figure 35 2 Dimensions Fluid Flow Schematics of Five Transverse Fractures Intersected by a Horizontal Well

Table 7 Time Consumption Comparison for 5 Fractures Case in 2 Dimensions Fluid Flow Schematics

Sub-Source Number	Rigorous Method (min)	Speed up Method (min)	Speed up Ratio
nx=1, nz=1 N=9	3.93	1.16	3.39
nx=2, nz=2 N=25	25.18	6.98	3.60

After providing a comparison of the program running time for the two methods, **Table 6** lists the computation time for the rigorous method and the modified method, corresponding to 3 fractures and various number of sub sources. We can see the modified method reduces the computation time by more than 50 %. Similarly, **Table 7** presents data for the 5 fractures case. For this case the modified method consumes less than one third of the time necessary for the rigorous method. Thus, we conclude that the modified method reduces the computation time by a factor approximately equal to the number of transverse fractures compared to the rigorous method.

3.7 Advanced Application – Asymmetric Wing Transverse Fractures Intersected by Curved Horizontal Well

We have developed both rigorous and speed-up method to deal with symmetric wing transverse fractures intersected by a horizontal well, as well as demonstrated the liability for both of the methods. In reality, the fractures are placed any position in the reservoir; the well could goes through any part of the fracture, not always from the center of the fracture. In advance, an innovative approach will be conducted to deal with more complex fracture well configuration. Sensitivity study included asymmetry of the fracture wing, well drainage area, as well as curved well. **Figure 36** shows the schematics of five transverse fractures with asymmetric wing intersected by a curved horizontal well.

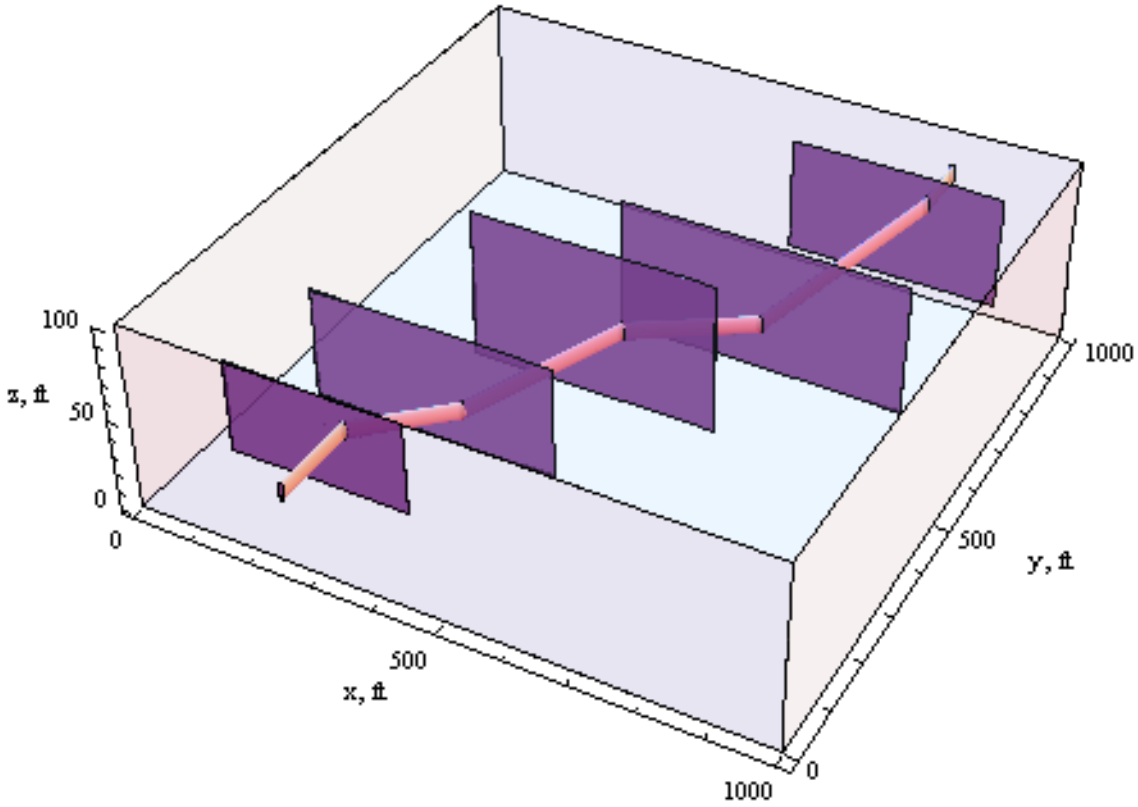

Figure 36 Schematics of Five Asymmetric Transverse Fractures Intersected by a Curved Horizontal Well

An example presented below to show the powerful function in forecasting well performance. Inside a no flow boundary, low permeability reservoir (k_x = 0.3 md, k_y = 0.3 md, k_z = 0.1 md), Five different sizes fractures are distributed in different positions. The summarized input parameters are shown in **Table 7**. **Table 8** summarizes the input parameters for horizontal well with five asymmetric transverse fractures intersected by a curved horizontal well. **Figure 37** presents the input interface for in the well performance software. **Figure 38** to **Figure 41** gives the forecasted productivity index, pressure value,

production rate, and cumulative production, in each time spot. The final result calculated is: Free gas: 682.6 mmscf.

Table 8 Summary of Input Parameters for Horizontal Well with Five Asymmetric Transverse Fractures Intersected by a Curved Horizontal Well

Reservoir parameters	Fracture No1 parameters	Fracture No2 parameters	Fracture No3 parameters	Fracture No4 parameters	Fracture No5 parameters
x_e = 1000 ft y_e = 1000 ft z_e = 100 ft k_x = 0.3 md k_y = 0.3 md k_z = 0.1 md P_{ini}=1000 psi P_{wf}=100 psi	Center location: Cx=200 ft Cy=150 ft Cz=30 ft Half length: w_x= 150 ft w_z=25 ft w_y=0.3 ft Fracture permeability: k_{fx}=60000 md Well Position: x_w=250 ft z_w=40 ft r_w=0.3 ft	Center location: Cx=300 ft Cy=300 ft Cz=40 ft Half length: w_x= 200 ft w_z=30 ft w_y=0.3 ft Fracture permeability: k_{fx}=60000 md Well Position: x_w=350 ft z_w=30 ft r_w=0.3 ft	Center location: Cx=450 ft Cy=500 ft Cz=50 ft Half length: w_x= 200 ft w_z=40 ft w_y=0.3 ft Fracture permeability: k_{fx}=60000 md Well Position: x_w=500 ft z_w=30 ft r_w=0.3 ft ft	Center location: Cx=650 ft Cy=650 ft Cz=50 ft Half length: w_x= 230 ft w_z=35 ft w_y=0.3 ft Fracture permeability: k_{fx}=60000 md Well Position: x_w=650 ft z_w=40 ft r_w=0.3 ft	Center location: Cx=750 ft Cy=900 ft Cz=60 ft Half length: w_x= 170 ft w_z=30 ft w_y=0.3 ft Fracture permeability: k_{fx}=60000 md Well Position: x_w=800 ft z_w=75 ft r_w=0.3 ft

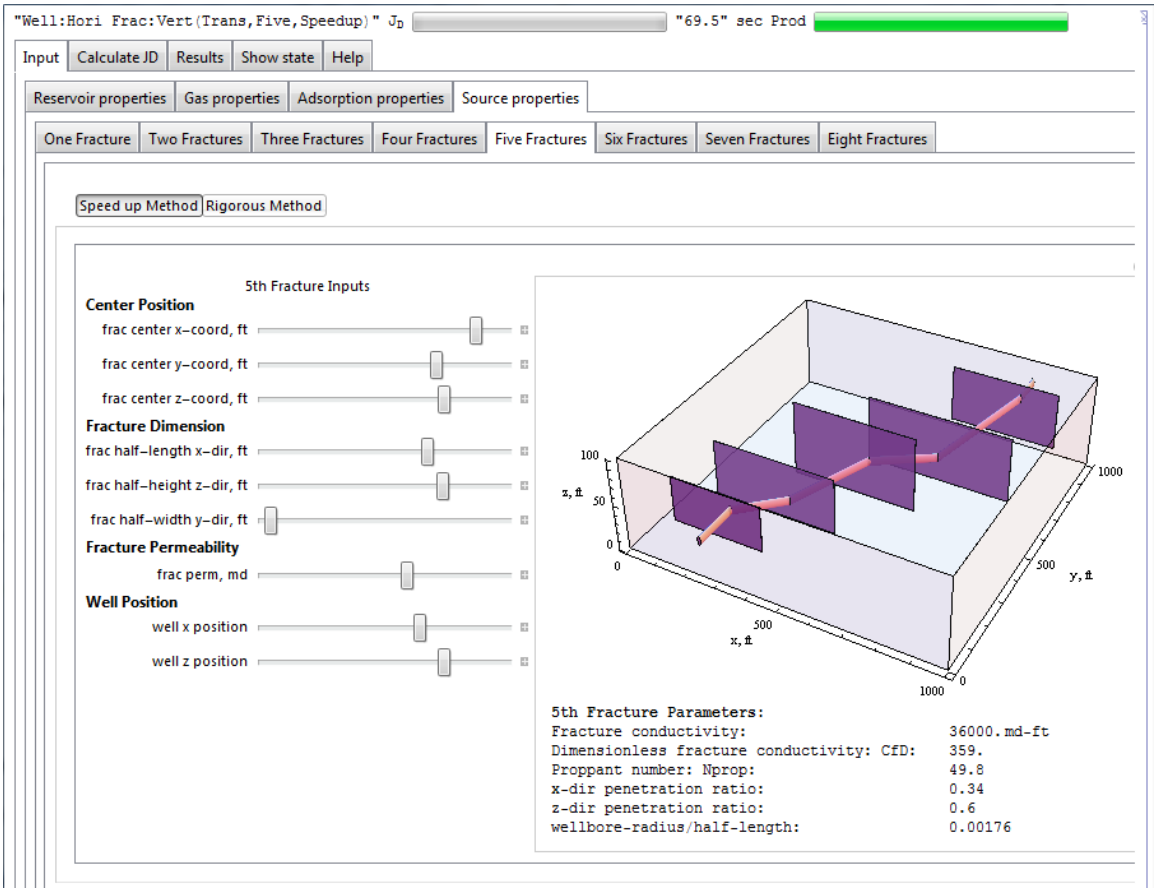

Figure 37 Interface of the Input Parameters for Horizontal Well with Five Asymmetric Transverse Fractures Intersected by a Curved Horizontal Well

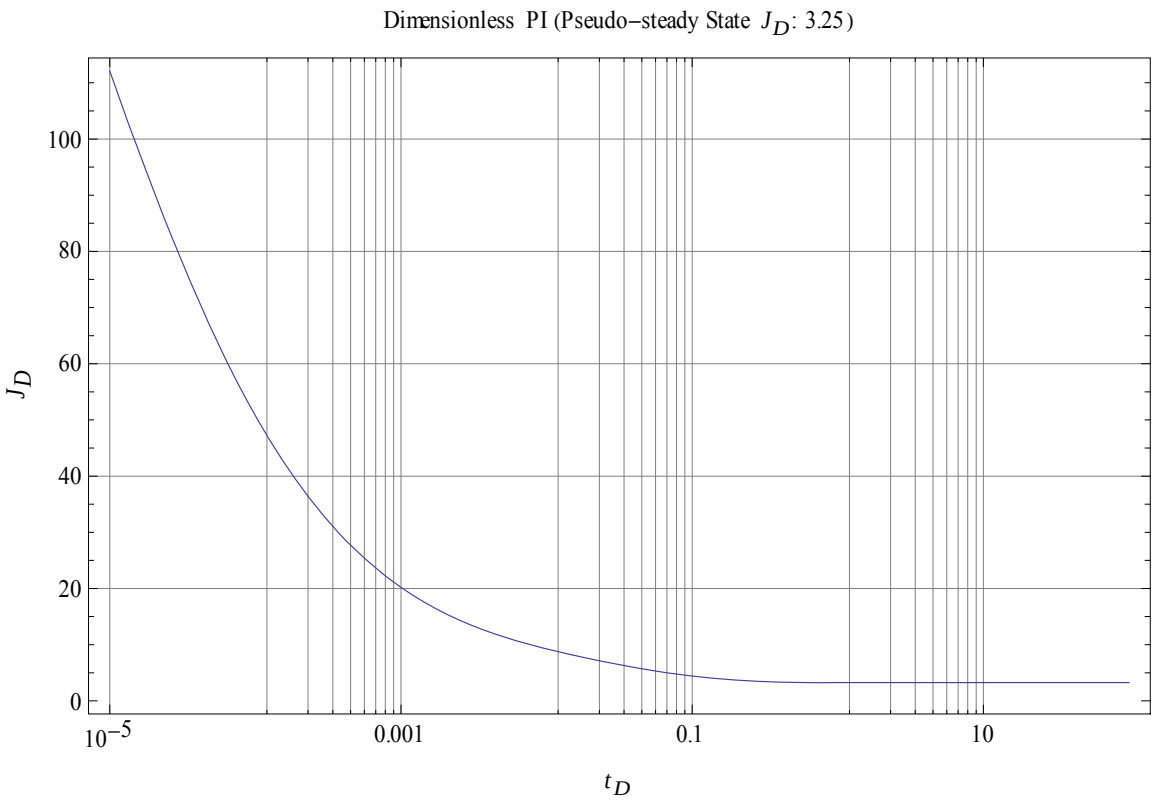

Figure 38 Dimensionless Productivity Index Forecast for Five Fractures Intersected by a Curved Horizontal Well

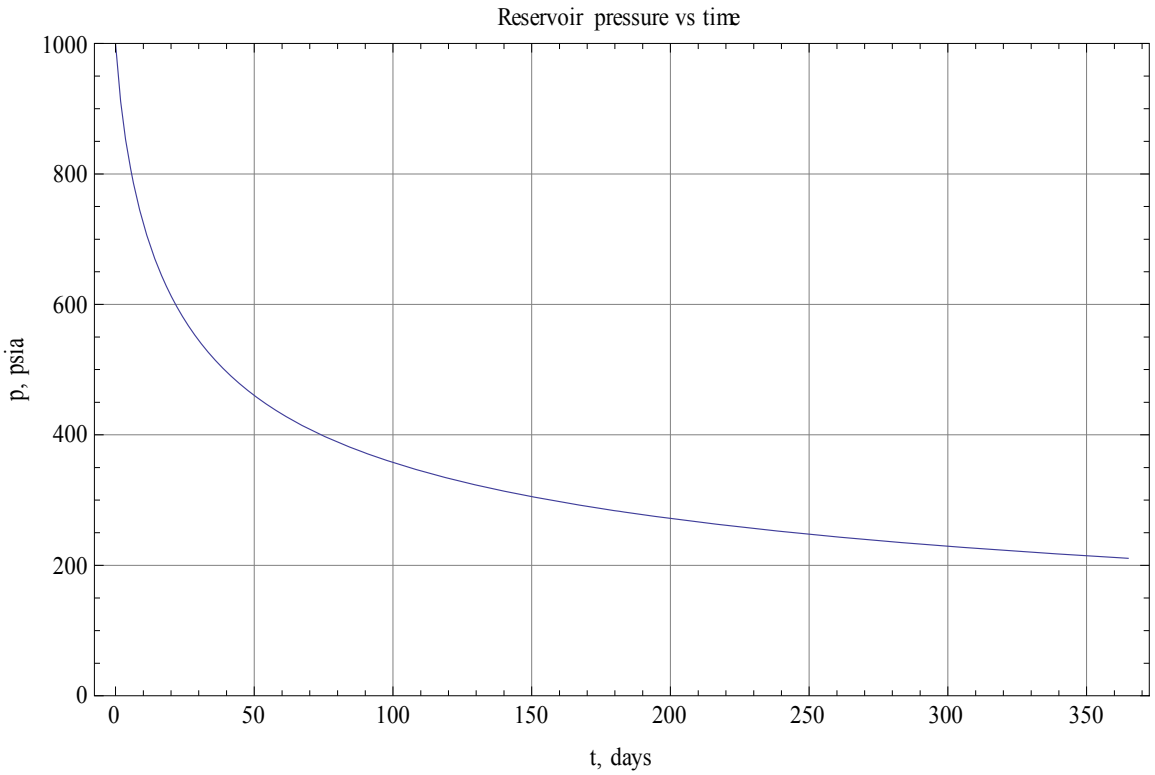

Figure 39 Pressure Forecasting for Five Fractures Intersected by a Curved Horizontal Well

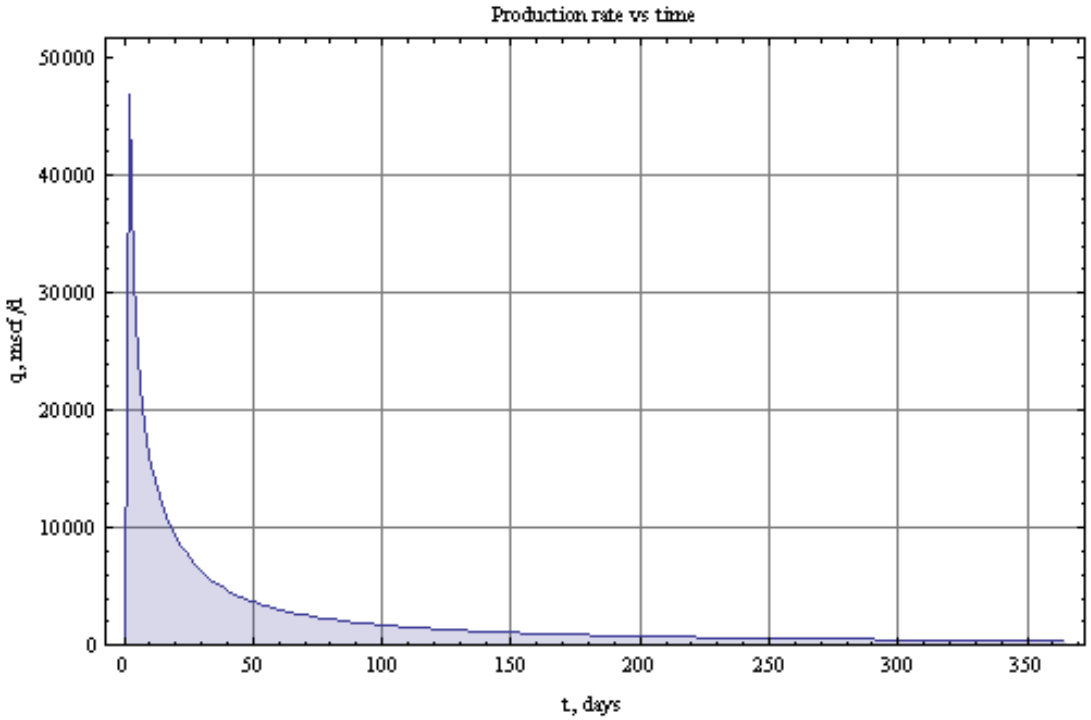

Figure 40 Production Rate Forecast for Five Fractures Intersected by a Curved Horizontal Well

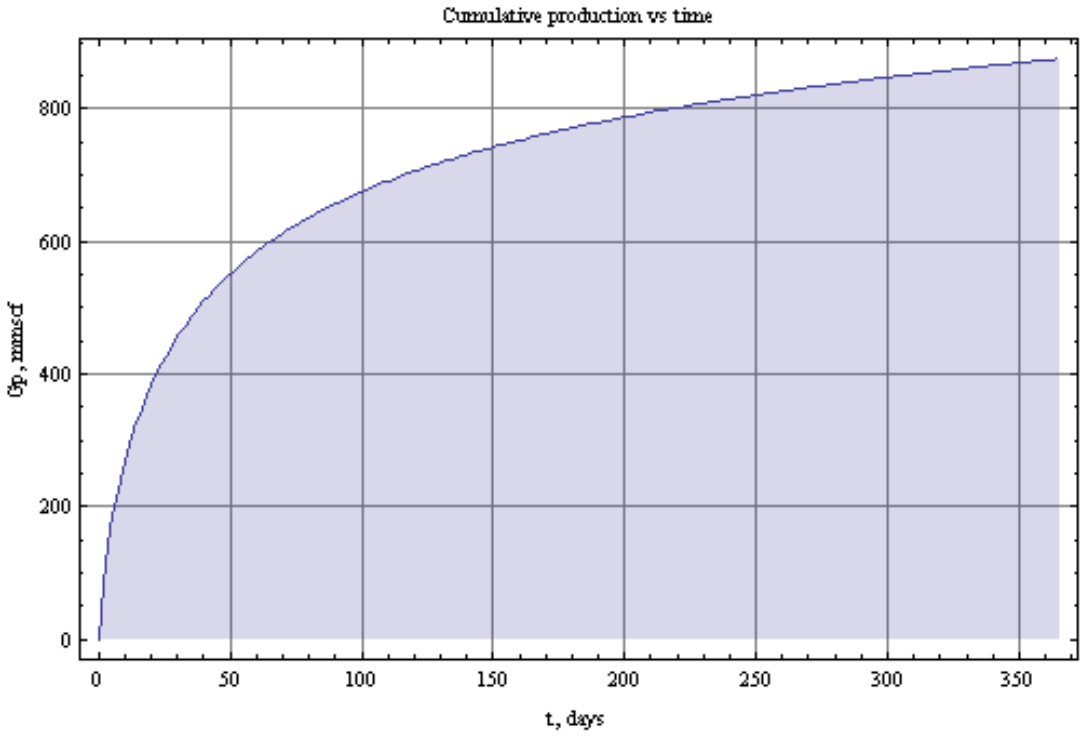

Figure 41 Cumulative Production Forecast for Five Fractures Intersected by a Curved Horizontal Well

3.8 Field Example Study

The Cotton Valley sandstone, located in north-central Louisiana and East Texas, is an extensive, coastal strand-plain sandstone deposition. Formation permeability and porosity are very low and stimulation is necessary in most Cotton Valley wells to obtain economic production. The depth of the formation is from 8,000 to 12,000 ft and the reservoir temperature is encountered from 230 to 280 F.

Several laboratory tests have been conducted on Cotton Valley sandstone samples from many areas in north central Louisiana and East Texas, The formation core samples are usually representative o; a medium-hard, gray sandstone reservoir. The physical appearance of the core varies with position in the interval.

The formation types examined ranged from sandstone with acid solubility of less than 5 percent to limey sand with acid volubility as high as 45 to 50 percent. The primary characteristics shared by the samples were the low porosities (less than 10%) (Jennings and Sprawls, 1977).

On September 13 and 14, 2007, Schlumberger provided StimMAP™ microseismic monitoring services for a six stage fracture treatment in the Cotton Valley Sand formation on the Burton A 17 well. The subject well is located in the South Carthage field, Panola County, Texas.

The monitoring well, Mason #16, is located 2,264.5 ft to the north and 1,296.3 ft to the east of the treatment wellhead. During the treatment, an array of eight geophones, with 100 ft between each sensor, monitored the microseismic activity.

Halliburton performed all the stimulation treatments on the Burton A 17 well and the information presented here is taken from their stimulation reports. A Peak completion system was run that comprised of ported sleeves placed within an uncemented liner in the lateral; external packers were placed between each sleeve to isolate the open hole between stages. Each sleeve is opened and isolated sequentially with the use of balls dropped from the surface. As a result, all the stages were pumped in a continuous system.

The map view, longitudinal view, and transverse view below, **Figure 42**, **Figure 43** and **Figure 44**, respectively, illustrate the final microseismic maps. Events are colored by stage number. **Figure 45** illustrates the relationship between the vertical extent of the recorded microseismic events and the lithology. **Figure 46** shows the location in a map view (Malpani et al., 2007).

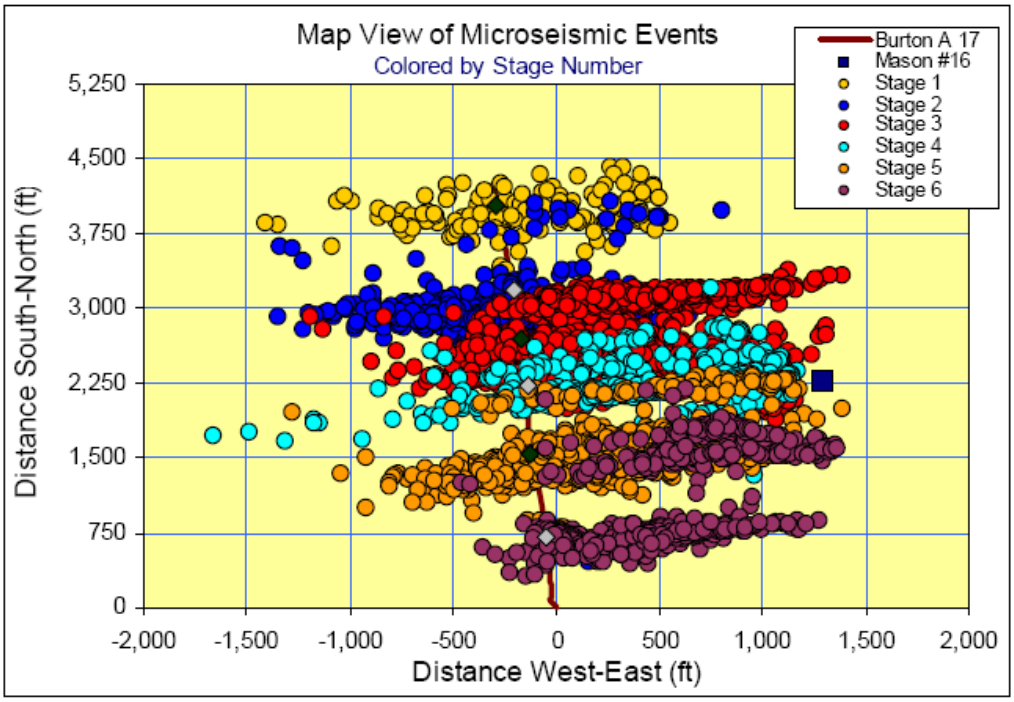

Figure 42 Map View (Length and Width)

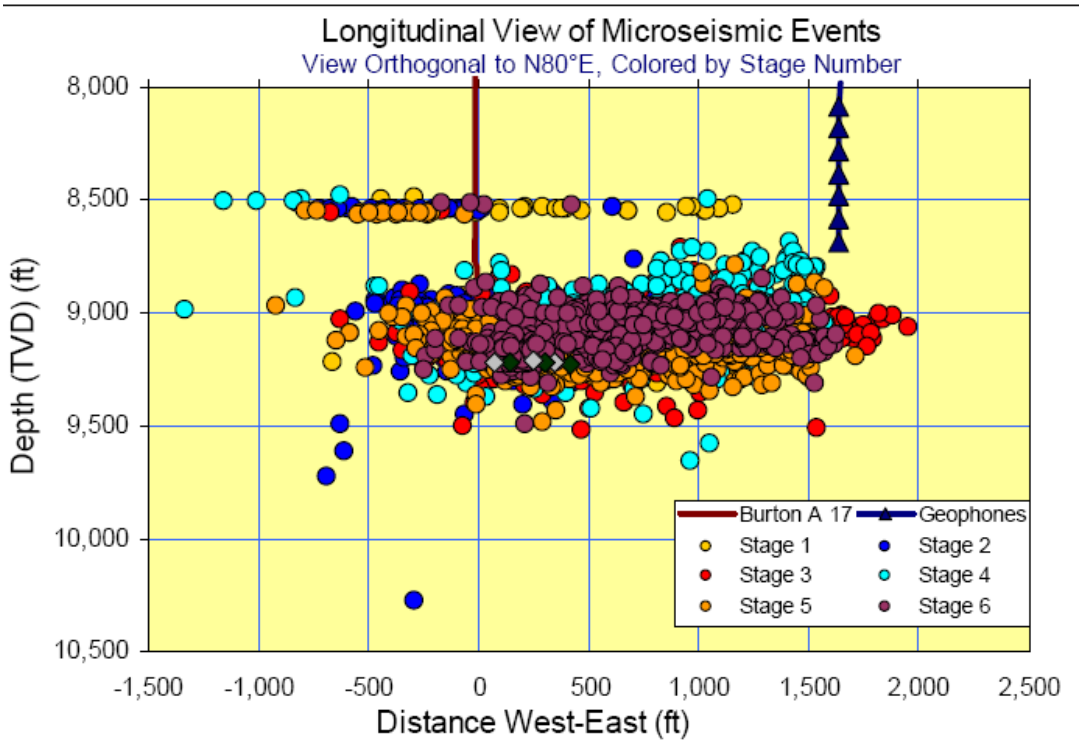

Figure 43 Longitudinal View (Length and Height)

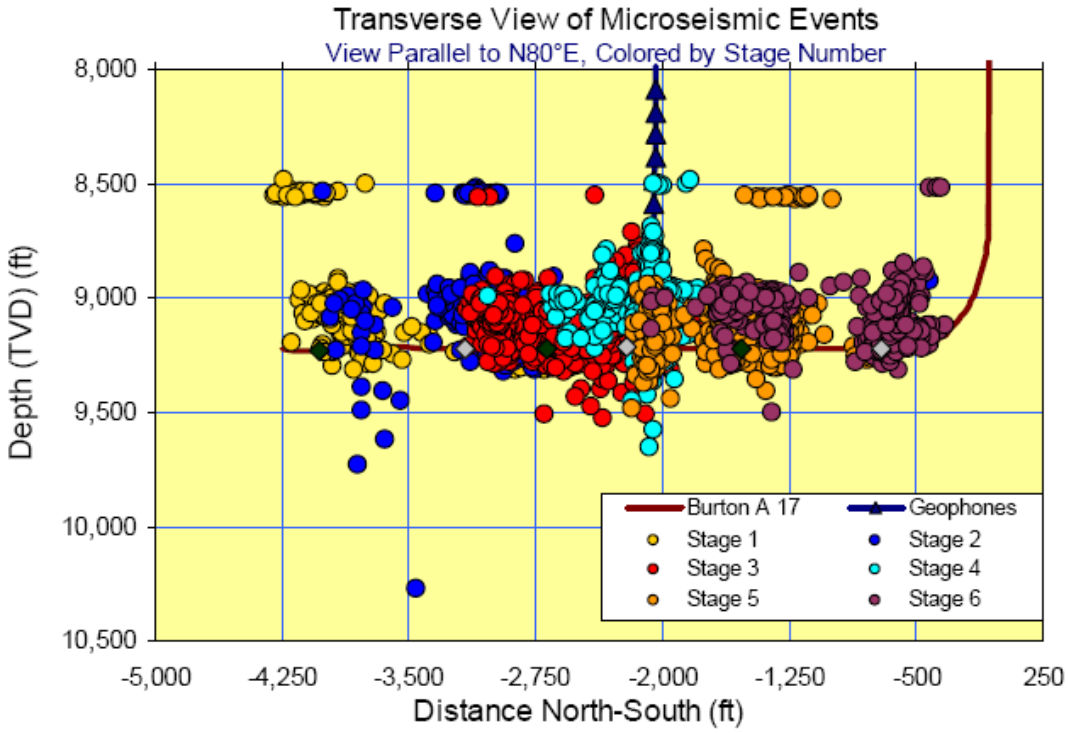

Figure 44 Transverse View (Height and Width)

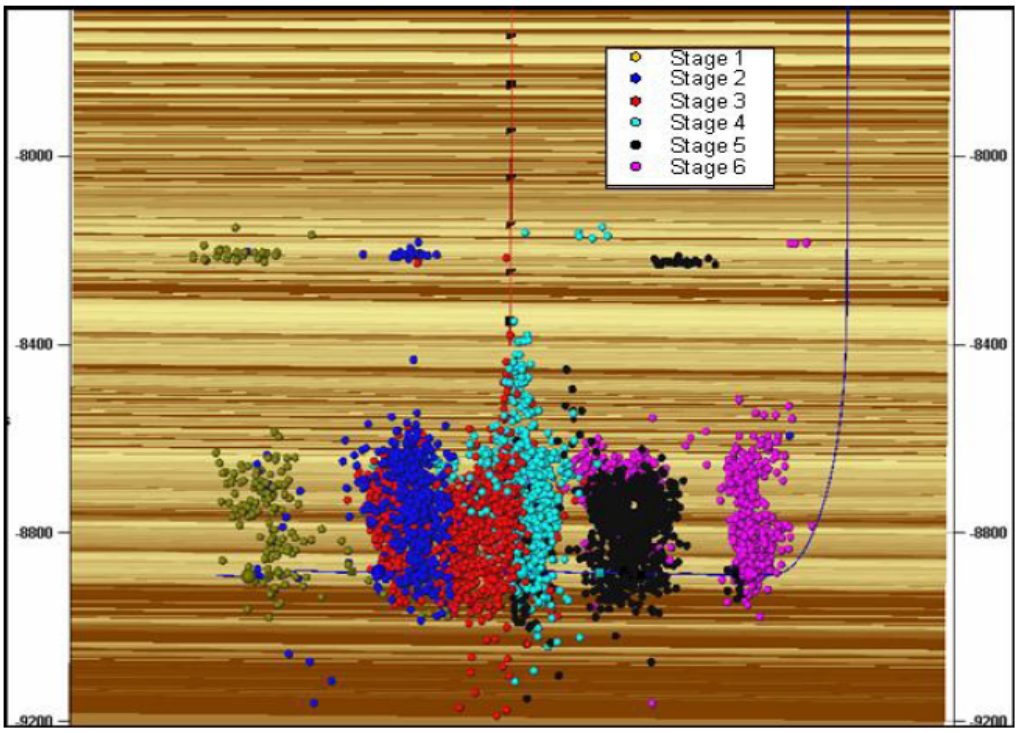

Figure 45 Lithology vs. Microseismic Events

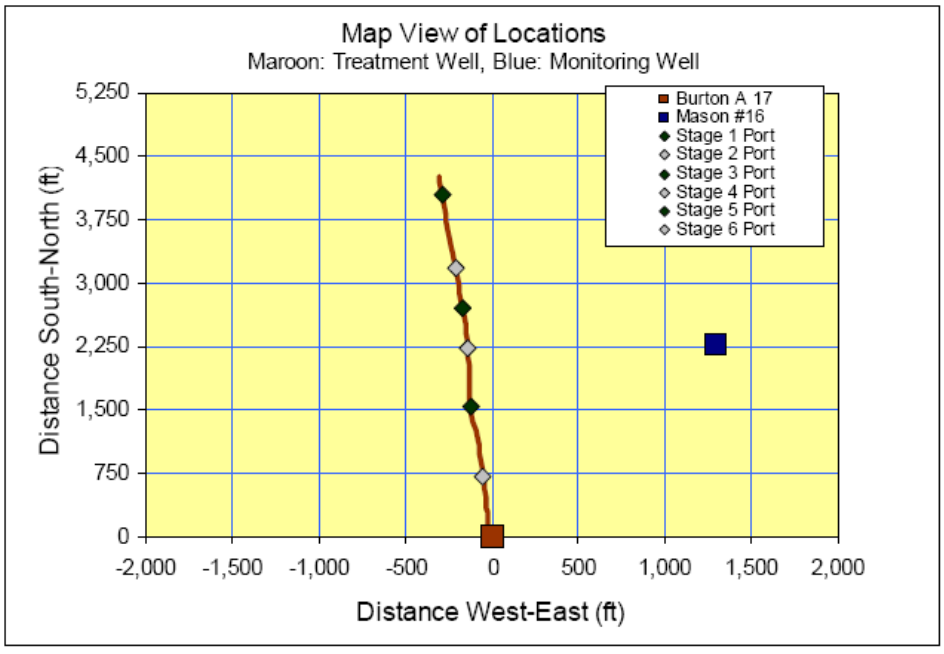

Figure 46 Map View of Treatment Well and Monitor Well Location

By monitoring the evolution of the microseismic events that occurred through time for a six stage fracture treatment in the Burton A 17 well, we determine the fracture geometry of each stage. This information guides the characterization of the reservoir and impact the design of future treatments in the field. In addition, determining the fracture azimuth is beneficial for the in-fill drilling program in the area.

This is a horizontal gas well located in the South Carthage field in Panola County, Texas. The completion details are summarized in **Table 9**.

Table 9 Completion Summary of the Burton A17 Well

Description	Value
Kelly Bushing (ft)	334
Formation	Cotton Valley Sand
Maximum Deviation (deg from Vertical)	93
Port Location for Stage 1 MD (ft)	12,984
Port Location for Stage 2 MD (ft)	12,117
Port Location for Stage 3 MD (ft)	11,634
Port Location for Stage 4 MD (ft)	11,163
Port Location for Stage 5 MD (ft)	10,466
Port Location for Stage 6 MD (ft)	9,642

By eliminating outliers, an interpretation of the fracture geometry can be provided. The dimensions are summarized in**Table 10**.

Table 10 Interpreted Microseismic Geometry

Description	Stage 1	Stage 2	Stage 3	Stage 4	Stage 5	Stage 6
Ported Sleeve MD (ft)	12,984	12,117	11,634	11,163	10,466	9,642
Azimuth	N80°E	N80°E	N80°E	N80°E	N80°E	N80°E
Total Length (ft)	1,158	1,544	2,158	1,839	1,929	1,255
Height (ft)	328	432	668	649	338	360
Top TVD (ft)	8,985	8,888	8,771	8,726	8,975	8,928
Bottom TVD (ft)	9,313	9,320	9,438	9,375	9,312	9,287
Length Along East Projection (ft)	792	818	1,481	1,285	1,382	1,046
Length Along West Projection (ft)	367	727	676	554	547	209
Equivalent Half-Length (ft)	579	772	1,079	920	965	627

Table 11 Input Parameters Summary of the Burton A17 Well

stage	1	2	3	4	5	6
Fracture	6	5	4	3	2	1
E-W, ft	270	190	152	122	108	33
well x, ft	73	153	191	221	235	310
well z, ft	678	678	678	678	678	678
N-S (ft)	3990	3137	2674	2199	1533	680
center y	3990	3137	2674	2199	1533	680
Length along east, ft	792	818	1481	1285	1382	1046
Length along west, ft	367	727	676	554	547	209
half x, ft	579.5	772.5	1078.5	919.5	964.5	627.5
half x, ft (modified)	72	97	135	115	121	78
center x	286	199	594	587	653	729
center x, ft (modified)	100	159	242	267	288	363
half x, ft	206	206	206	206	206	206
center x	206	206	206	206	206	206
top	8985	8888	8771	8726	8975	8928
bottom	9313	9320	9438	9375	9312	9287
half z	164	216	334	325	169	180
center z	751	796	796	850	757	793

From the Texas Railroad Commission, the production data, as shown in **Table 11**, could be found by use of the API number. Production Data Curve is shown in **Table 12**, and is drawn in **Figure 47**, starting from 9/1/2007. The speedup multiple fracture DVS well performance program forecasts the production rate as shown in **Figure 48**.

Table 12 Production Data Starting from 9/1/2007

Date	Day	Gas
9/1/2007	0	68720
10/1/2007	30	96342
11/1/2007	60	73618
12/1/2007	90	56732
1/1/2008	120	50470
2/1/2008	150	43578
3/1/2008	180	45303
4/1/2008	210	39649
5/1/2008	240	38739
6/1/2008	270	36524
7/1/2008	300	37080
8/1/2008	330	35668
9/1/2008	360	28324
10/1/2008	390	30881
11/1/2008	420	28459
12/1/2008	450	28716
1/1/2009	480	28730
2/1/2009	510	22070
3/1/2009	540	25090
4/1/2009	570	25423
5/1/2009	600	25455
6/1/2009	630	23014
7/1/2009	660	23147

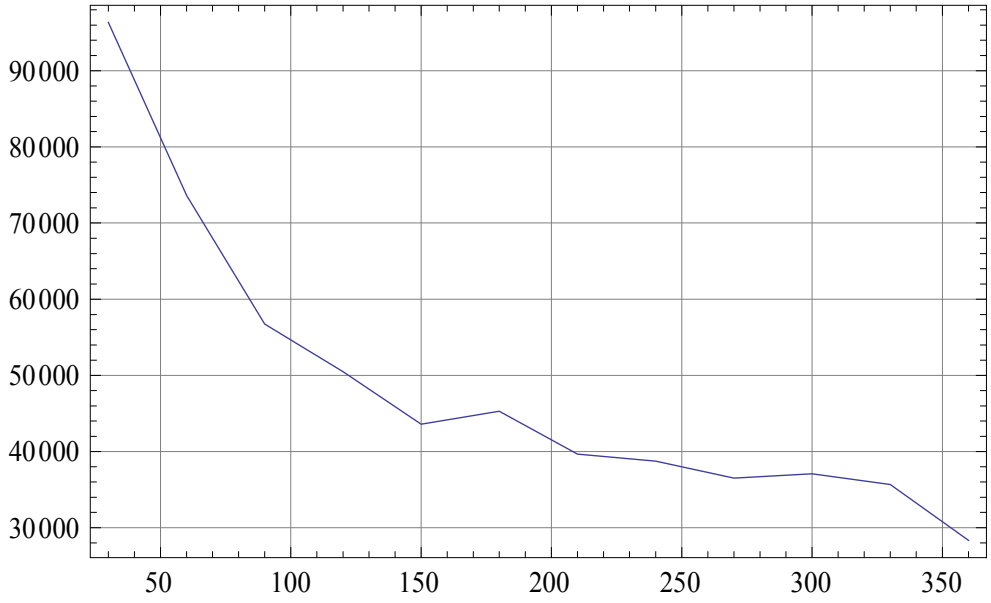

Figure 47 Production Data Curve Starting from 9/1/2007

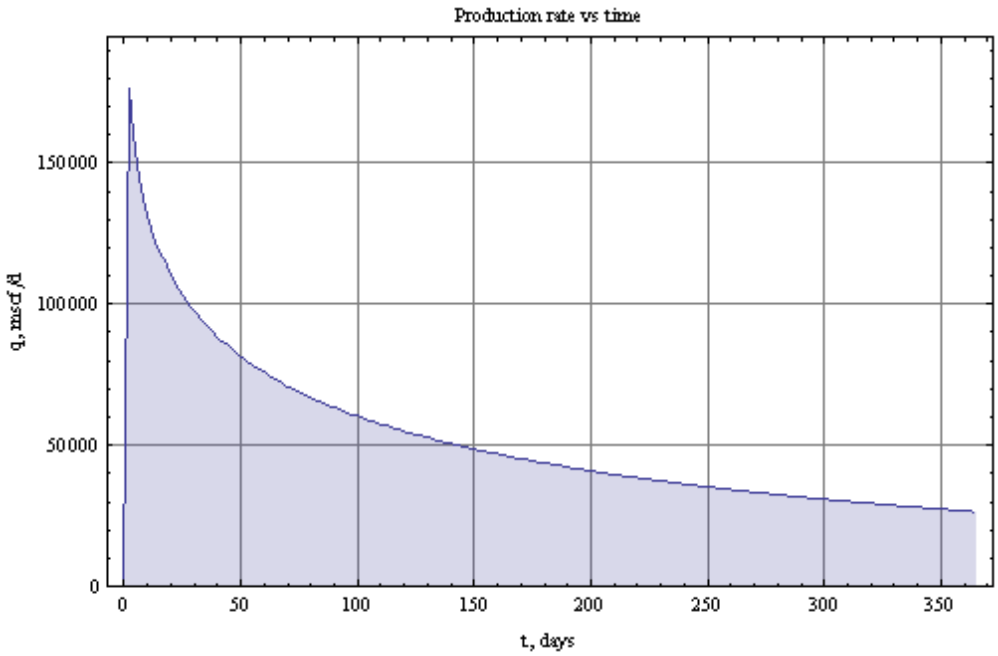

Figure 48 Production Rate Forecasted from Speedup Multiple Fracture DVS Method

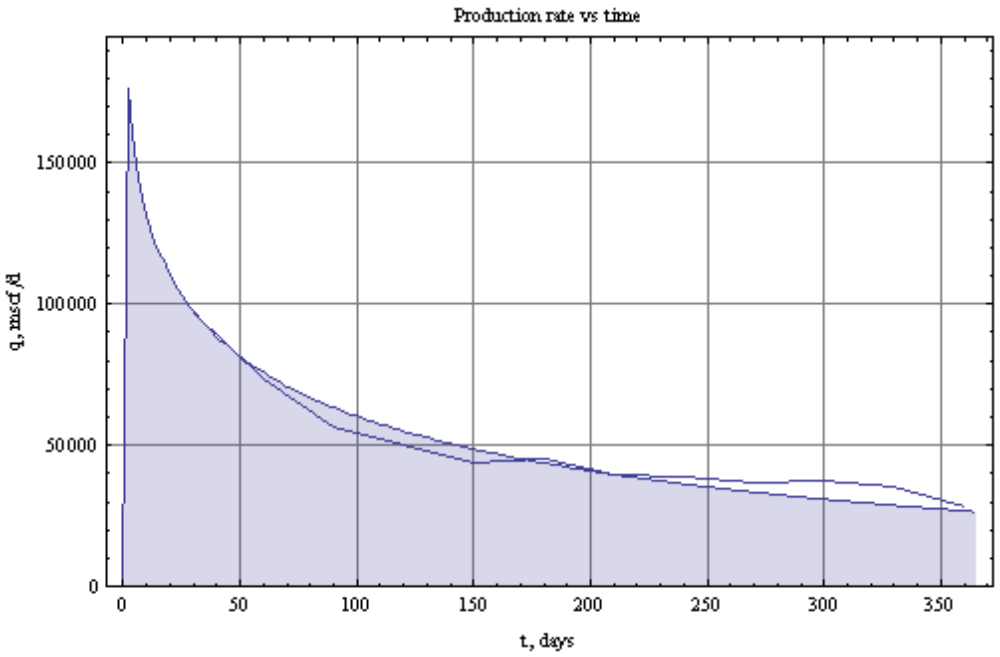

Figure 49 Comparison of Forecasted Production Rate with Field Production Data

We can see, from **Figure 49**, that in the transient flow period, forecasted production rate from DVS multiple fractures simulator stands a good agreement with results from actual field data. In the pseudo-stady state period, there presents an acceptable error for the simulated production value.

CHAPTER IV

SUMMARY AND CONCLUSIONS

4.1 Summary

The primary purpose of this work is based on the DVS theory to develop a method to predict the transient and pseudosteady-state pressure and production behavior of a closed, rectangular reservoir. In this work, the following tasks are performed:

- We develop a rigorous and innovative speed-up well performance model, based on DVS method, to calculate the dimensionless productivity index J_D for the horizontal well intercepted by multiple fractures.
- We validate the results from rigorous simulator for well testing and production forecast by comparing the results with simple symmetric well and fracture configuration.
- We validate the applicability and demonstrate the advantage of the solution from speed-up simulator for the horizontal well intercepted by multiple fractures with the rigorous simulator.
- We show the capability of the speed up production simulator to handle more complicated well/fracture configurations. Sensitivity study included well drainage size, asymmetry of the fracture wings, and curved well.
- We conduct field example studies using the production data and stimulation treatment data of gas wells from East Texas Cotton Valley formation and Barnett Shale.

4.2 Conclusion

In this work, we introduced an approach to produce consistent transient and pseudo-steady state solutions in a rigorous way, for the configuration of multiple transverse fractures intercepted by a horizontal well. Furthermore, we developed a speedup method to deal with multiple transverse fractures within reduced computational time. This speedup method is validated through comparison both to rigorous method solution for simple symmetric fracture configuration, and to field production data for complex well/fracture configuration. It provides reliable results with relatively moderate computational effort. The advantage of the speedup method is more obvious when applied to a system with increasing complexity, such as fracture number. The speedup method has the ability to provide a consistent transient and pseudosteady state productivity index solution, which makes it a promising optimization and screening tool for completion schemes involving multiple fractures.

4.3 Recommendations for Future Work

We showed one case study for the application of speedup method. The future work on this topic could focus on exploring more applications on the innovative method. The speedup method reduces computational time in a considerable portion. The future work would take advantage of this method into network fracture problems.

The assumption in development of the solution was that the reservoir had the homogeneous properties, such as: permeability, porosity, water saturation etc; the reservoir had a closed boundary; the fracture wing should not be much longer than the distance between fractures. The future work could also be directed to eliminate these limited assumptions.

REFERENCES

Amini, S. 2007. Development and Application of the Method of Distributed Volumetric Sources to the Problem of Unsteady State Fluid Flow in Reservoirs, Ph.D. dissertation, Texas A&M University.

Azar-Nejad, F., Tortike, W.S., and Farouq Ali. S.M. 1996a. Potential Distribution around the Sources with Finite Length (Horizontal, Vertical Partially Penetrating Wells and Fractures) Part II: Transient Flow. Paper SPE 35269 presented at the Mid-Continent Gas Symposium, Amarillo, Texas, 28–30 April.

Azar-Nejad, F., Tortike, W.S., and Farouq Ali. S.M. 1996b. Potential Distribution around the Sources with Finite Length (Horizontal, Vertical Partially Penetrating Wells and Fractures) Part I: Steady State Fluid Flow. Paper SPE 35270 presented at the Mid-Continent Gas Symposium, Amarillo, Texas, 28–30 April.

Baihly, J., Coolidge, A., Dutcher, S., Villarreal, R., Craven, M., Brook, K., and Le Calvez, J.H. 2007. Optimizing the Completion of a Multilayer Cotton Valley Sand Using Hydraulic-Fracture Monitoring and Integrated Engineering. Paper 110068 presented at the SPE Annual Technical Conference and Exhibition, Anaheim, California, 11-14 November.

Baihly, J., Grant,D., Fan, L., and Bodwadkar, S. 2009. Horizontal Wells in Tight Gas Sands--A Method for Risk Management to Maximize Success. *SPE Production & Operations* **24** (2): 277-292, SPE-110067-PA

Chen, H.Y. and Asaad, N. 2005. Horizontal-Well Productivity Equations with Both Uniform-Flux and Uniform-Pressure Wellbore Models. Paper SPE 97190 presented at the SPE Annual Technical Conference and Exhibition, Houston, Texas, 9–12 October.

Cinco-Ley, H. and Meng, H.-Z. 1988. Pressure Transient Analysis of Wells With Finite Conductivity Vertical Fracture in Double Porosity Reservoirs. Paper SPE 18172 presented at the SPE Annual Technical Conference and Exhibition, Houston, Texas, 2–5 October.

Cinco-Ley, H., Ramey, H.J. Jr., and Miller, F.G. 1975. Unsteady-State Pressure Distribution Created by a Well with an Inclined Fracture. Paper SPE 5591 presented at Fall Meeting of the Society of Petroleum Engineers of AIME, Dallas, Texas, 28 September - 1 October.

Cinco-Ley, H. and Samaniego-V. F., 1981. Transient Pressure Analysis for Fractured Wells. *SPEJ* **33** (9): 1749–1766. SPE-7490-PA.

Cinco-Ley, H., Samaniego-V. F., and Domínguez, N. 1978. Transient Pressure Behavior of a Well with a Finite-Conductivity Vertical Fracture. *SPEJ* **18** (4): 253–264. SPE-6014-PA.

Economides, M.J., Oligney, R.E., and Valkó, P. P. 2002. *Unified Fracture Design, 23*-38. Alvin, Texas: Orsa Press.

Garbut, D., 2004. Unconventional Gas. Brochure, Houston, Texas: Schlumberger

Gringarten, A.C. and Ramey, H.J. Jr. 1973. The Use of Source and Green's Functions in Solving Unsteady-Flow Problems in Reservoirs. *SPEJ* **13** (5): 285-296; Trans., AIME, 255. SPE-3818-PA

Gringarten, A.C., Ramey, H.J. Jr. and Raghavan, R. 1975. Applied Pressure Analysis for Fractured Wells. *SPEJ* **27** (7): 887-892, SPE-5496-PA

Jennings A.R. Jr. and Sprawls, B.T. 1977. Successful Stimulation in the Cotton Valley Sandstone - A Low-Permeability Reservoir. *JPT* **29** (10): 1267-1276, SPE-5627-PA

Le Calvez, J.H., Klem, R.C., Bennett, L., Erwemi, A., Craven, M. and Palacio, J.C. 2007. Real-Time Microseismic Monitoring of Hydraulic Fracture Treatment: A Tool to Improve Completion and Reservoir Management. SPE 106159 presented at the SPE Hydraulic Fracturing Technology Conference, College Station, Texas, 29-31 January

Malpani, R., Craven, M., Appelt, M., Brook, K. and White, D.J. 2007. StimMAP Evaluation Hydraulic Fracture Stimulation Monitoring Prepared for Devon Energy, South Carthage Field, Panola County, Texas.

Meyer, B.R. and Jacot, R.H. 2005. Pseudosteady-State Analysis of Finite-Conductivity Vertical Fractures. Paper SPE 95941 presented at the SPE Annual Technical Conference and Exhibition, Dallas, Texas, 9–12 October.

Valkó, P. P. User's Manual for Gas14.nb, April 2008.

Valkó, P. P. and Amini, S. 2007. The Method of Distributed Volumetric Sources for Calculating the Transient and Pseudo-steady State Productivity of Complex Well-Fracture Configurations. Paper SPE 106729 presented at the 2007 SPE Hydraulic Fracturing Technology Conference, College Station, Texas, 29-31 January

Warpinski, N.R., Wolhart, S.L, and Wright, C.A. 2001. Analysis and Prediction of Microseismicity Induced by Hydraulic Fracturing. Paper SPE 71649 presented at the SPE Annual Technical Conference and Exhibition, New Orleans, Louisiana, 30 September-3 October

Wong, D.W., Harrington, A.G. Jr. and Cinco-Ley, H. 1986. Application of the Pressure Derivative Function in the Pressure Transient Testing of Fractured Wells. *SPEFE* **1** (5): 470-480, SPE-13056-PA

VITA

Name:	Diangeng Fan
Born:	Anhui, China
Permanent Address:	Harold Vance Department of Petroleum Engineering, 3116 TAMU, College Station, TX 77841
Email Address:	fdgeng1985@gmail.com
Education:	B.S., Physics, University of Science and Technology of China, 2007 M.S., Petroleum Engineering, Texas A&M University, 2010